

CERES Angular Distribution Model Working Group Report

Lusheng Liang¹
Lusheng.Liang@nasa.gov

Sergio Sejas² Zachary Eitzen²

1. Analytical Mechanics Associates, Inc., Hampton, VA
2. ADNET Systems, Inc., Hampton, VA
3. NASA Langley Research Center, Hampton, VA

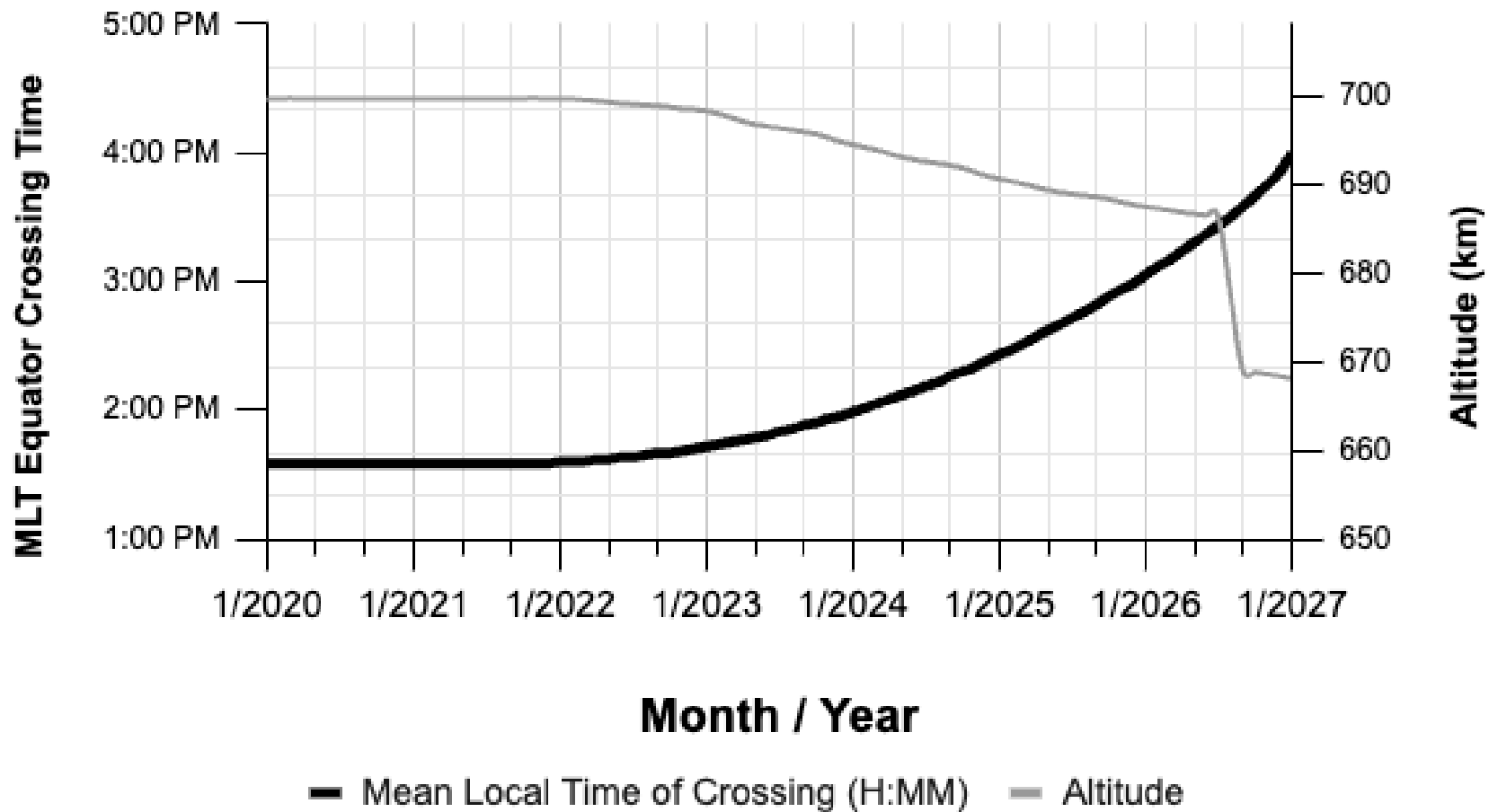
CERES Science Team Meeting, May 12-14, 2026
NASA Langley Research Center, Hampton, VA

Outline

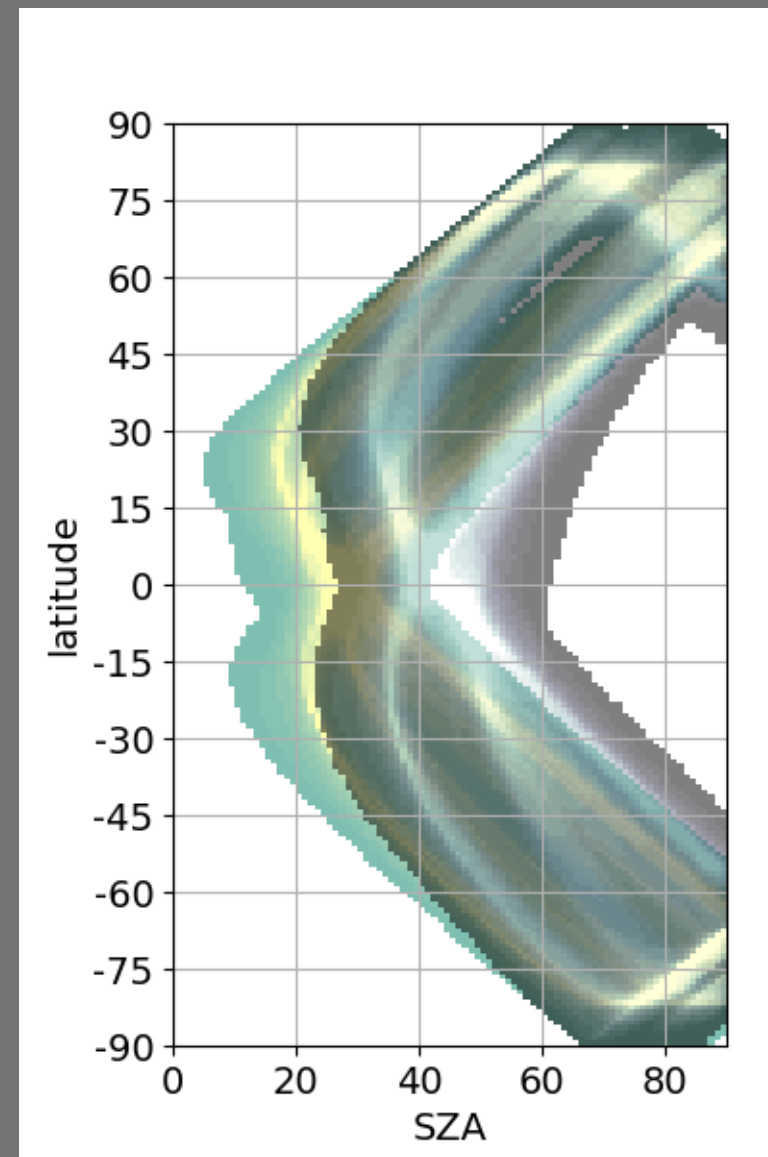
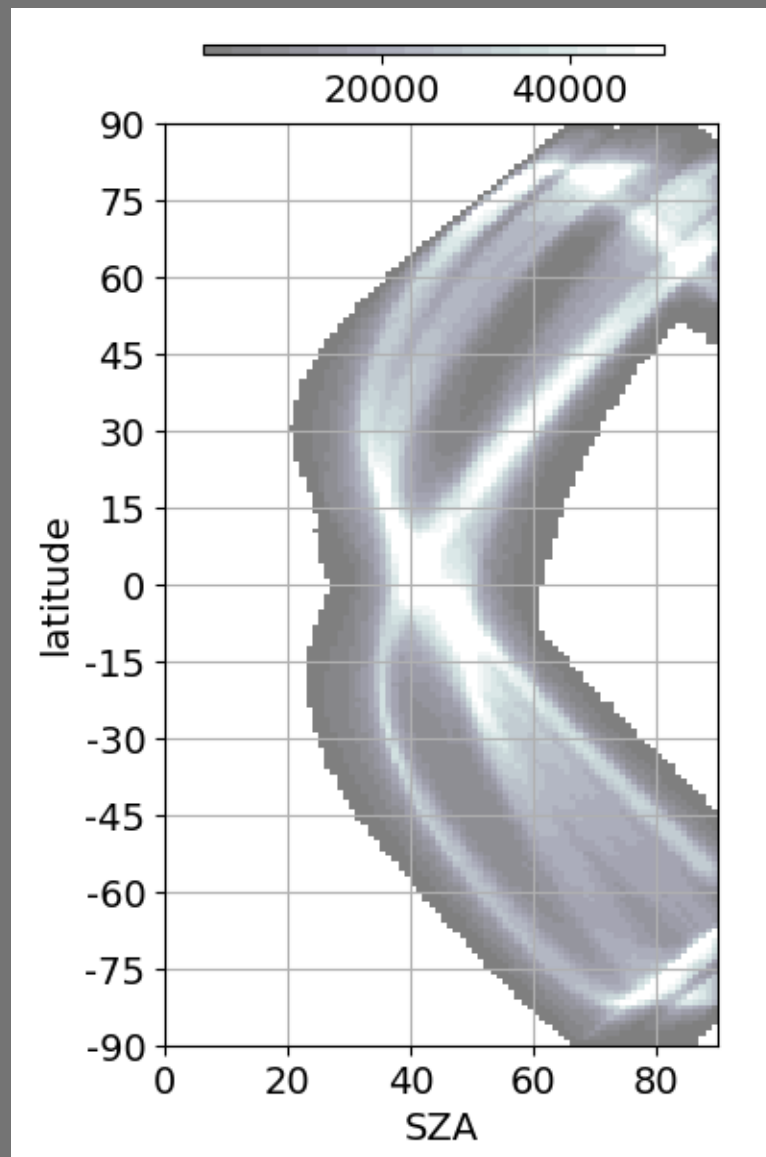
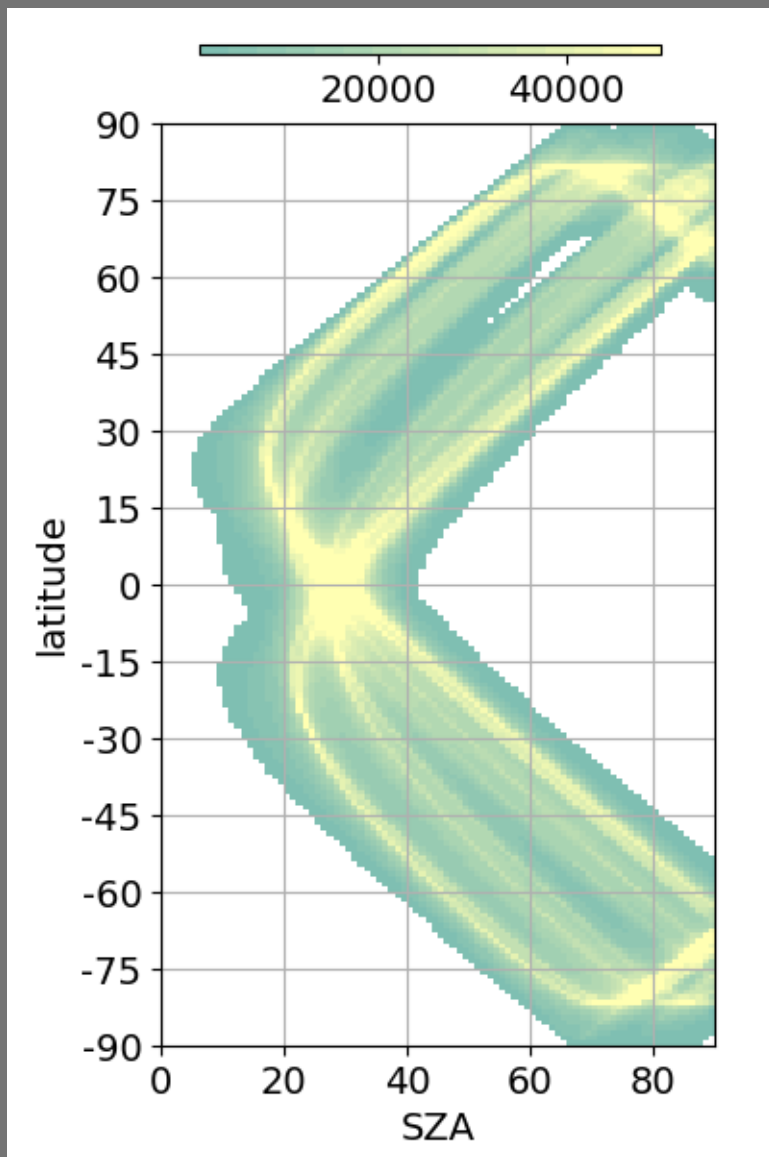
- Impact of Terra/Aqua orbital drifting on the CERES ADMs
- LUT approach for Split-SW flux retrieval

Impact of Terra/Aqua orbital drifting on the CERES ADMs

Estimated Future Changes to Aqua's Equator Crossing Time and Altitude



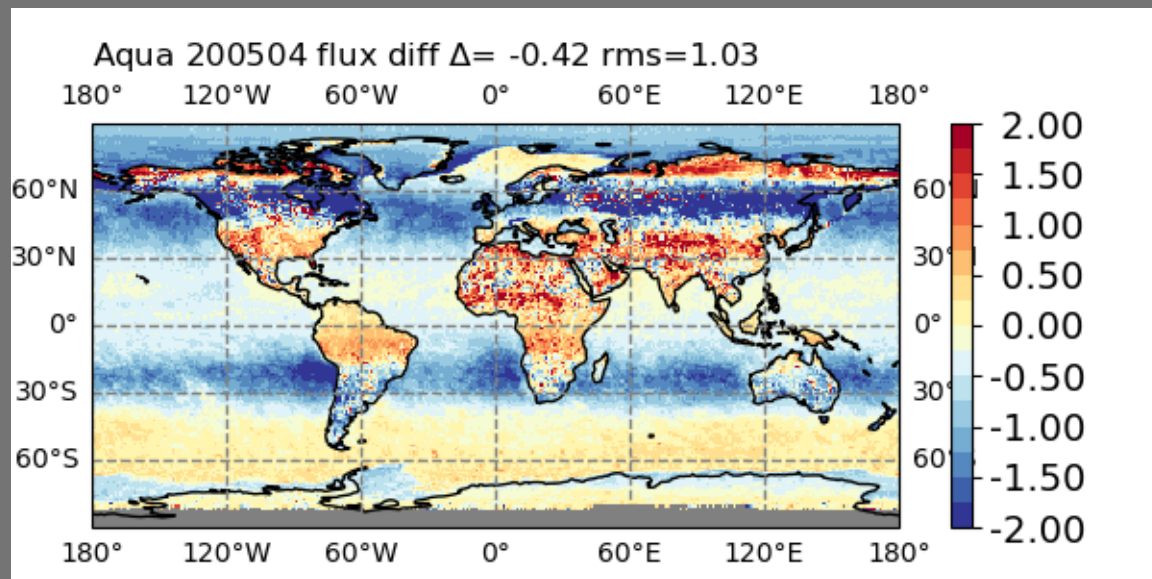
AQUA SZA sampling counts collected in 2004 Jan, Apr, Jul, and Oct



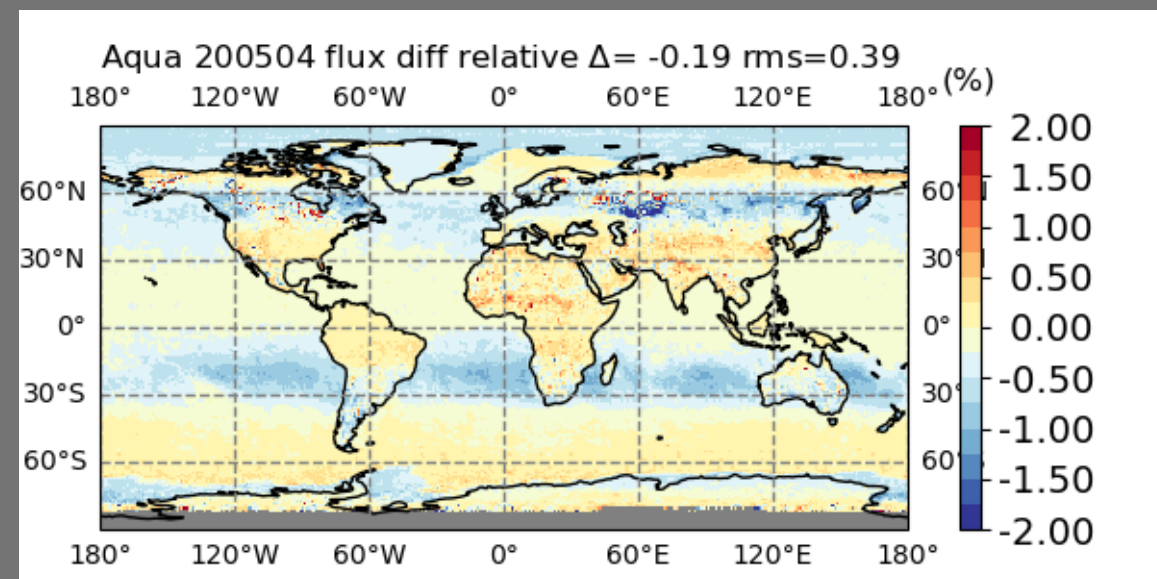
ADMs

- Aqua Edition 4 ADMs were constructed from cross-track and RAPs data from Aug 2002 to Mar 2005.
- A set of new ADMs is constructed by adding additional ~2.5 years of Aqua-FM3 RAPs data from Apr 2023 to Nov 2025.

Flux differences



Flux Relative differences



From radiance to flux: angular distribution models

- Sort observed radiances into angular bins over different scene types and calculate the averages:

$$\hat{I}(\theta_o, \theta, \phi)$$

- Integrate radiances to get flux:

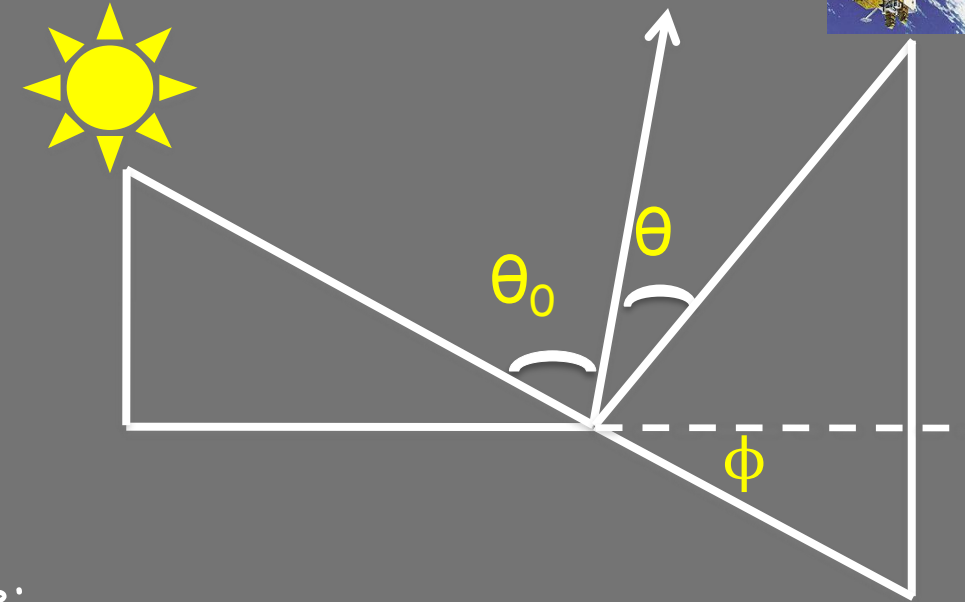
$$\hat{F}(\theta_o) = \int_0^{2\pi} \int_0^{\pi/2} \hat{I}(\theta_o, \theta, \phi) \cos\theta \sin\theta d\theta d\phi$$

- Estimate the anisotropic factor for each scene type:

$$\hat{R}(\theta_o, \theta, \phi) = \frac{\pi \hat{I}(\theta_o, \theta, \phi)}{\hat{F}(\theta_o)}$$

- For each radiance measurement, apply scene type dependent anisotropic factor to observed radiance to derive TOA flux:

$$F(\theta_o) = \frac{\pi I^o(\theta_o, \theta, \phi)}{\hat{R}(\theta_o, \theta, \phi)}$$



One of basis of ADMs is the averaging of radiances in a finite bin.
Are the radiance sampled well? Alternatively, to what extent is the mean radiance close to the truth?

Radiance Margin of Error (MoE)

Given a set of radiances in an ADM bin, the MoE can be estimated as

$$E = t^* \times \left(\frac{s}{\sqrt{n}} \right)$$

$$\frac{s}{\sqrt{n}}$$

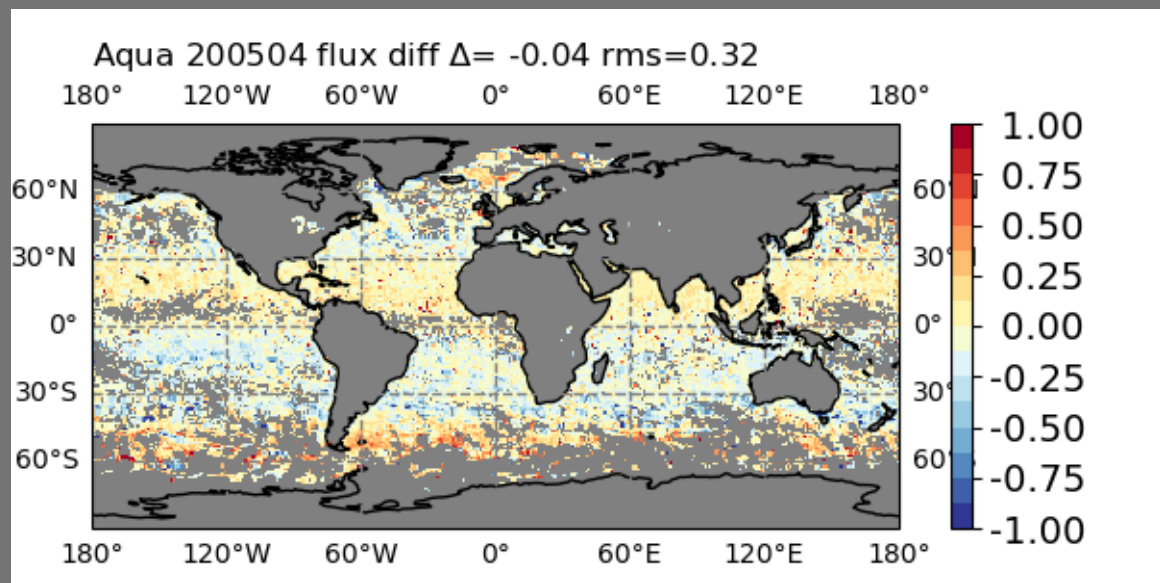
is the standard error calculated from standard deviation and sampling counts.

critical t^* value is calculated from the Student's t-test depending on the number of samples and pre-set significant level (usually, it is 5%).

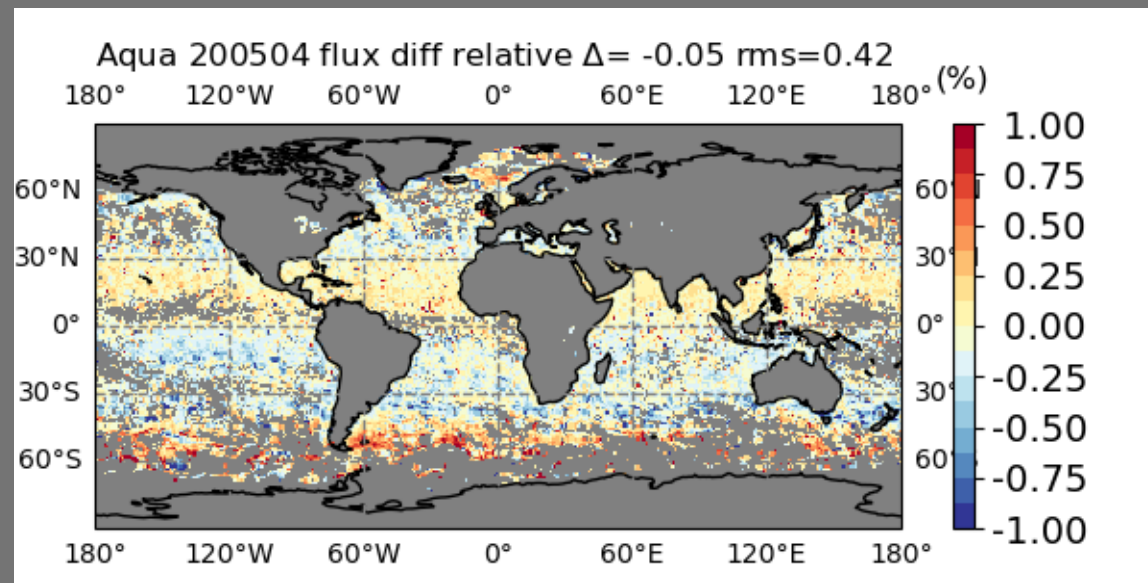
The confidence interval = estimated mean \pm E
(the estimated mean is within the interval for 95% of time to the truth).

Clear-sky over ocean

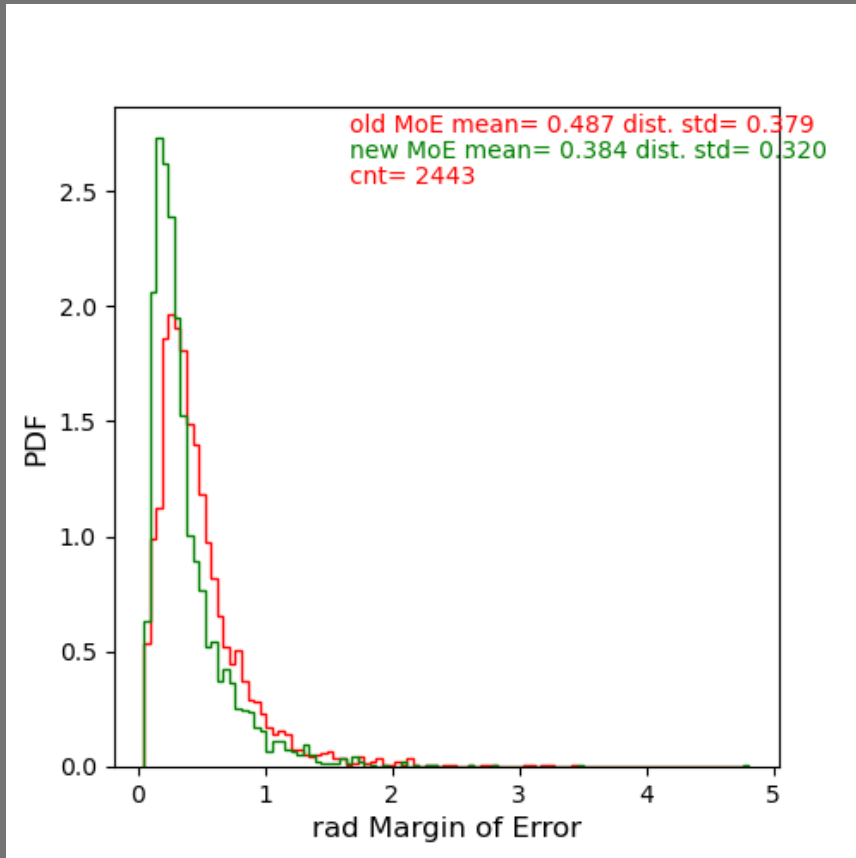
Flux differences



Flux Relative differences

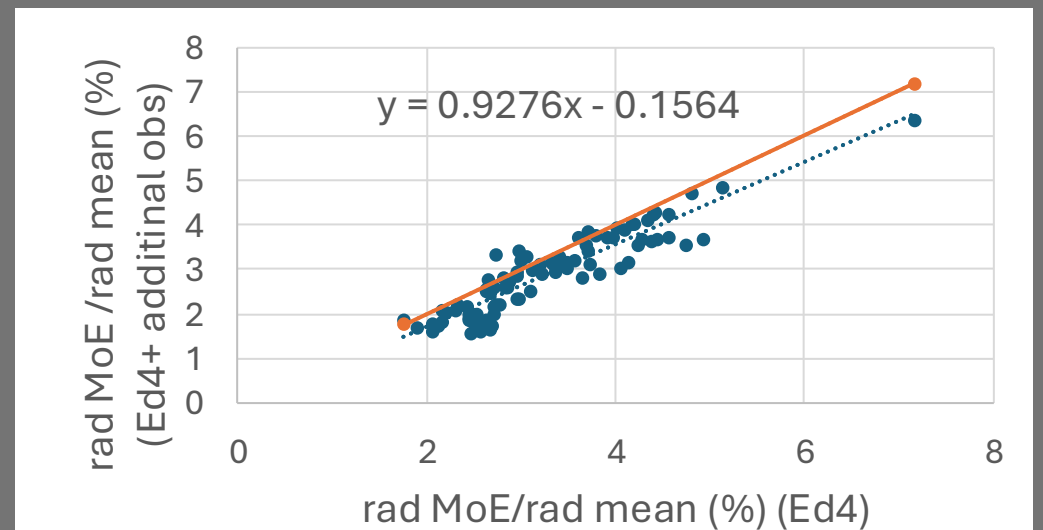
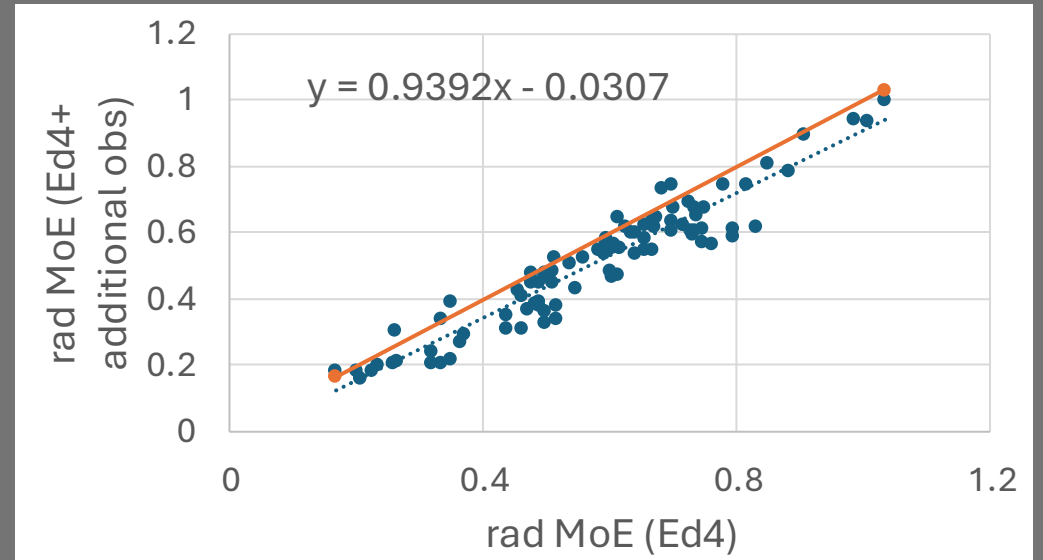


Clear-sky over ocean



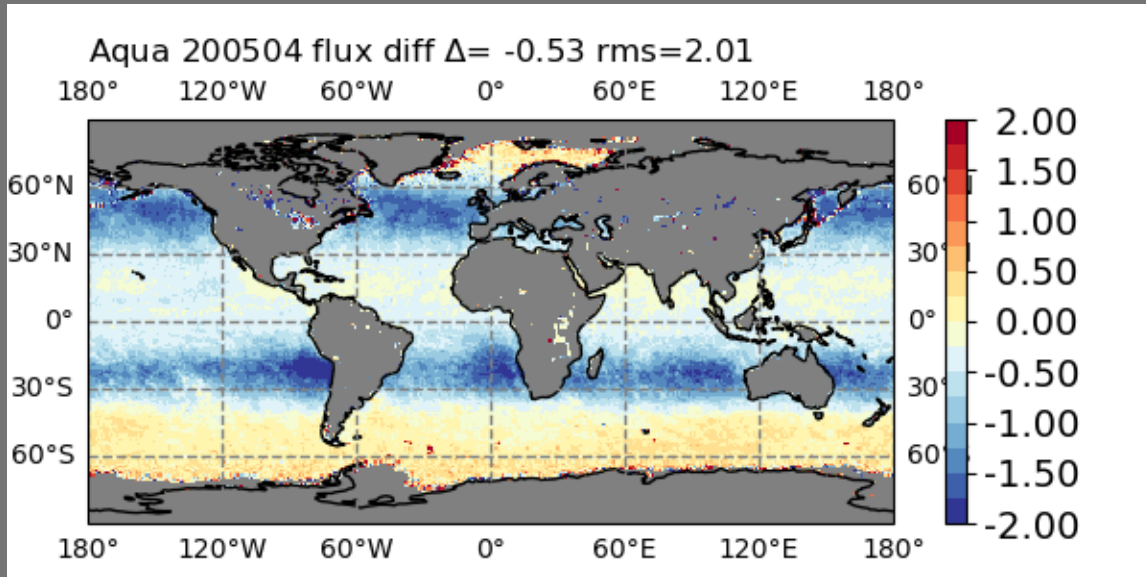
MoE distribution across viewing angles (45 VZA x 90 RAZ) for SZA = 38-40, ocean wind-speed=4-6 m/s, coarse model aerosols, and sampling counts > 10 in each viewing angle.

Collect mean MoE values from the MoE distributions for 7 SZA bin intervals from 15 to 71, 6 ocean wind speed bins, and both coarse model and fine model aerosols.

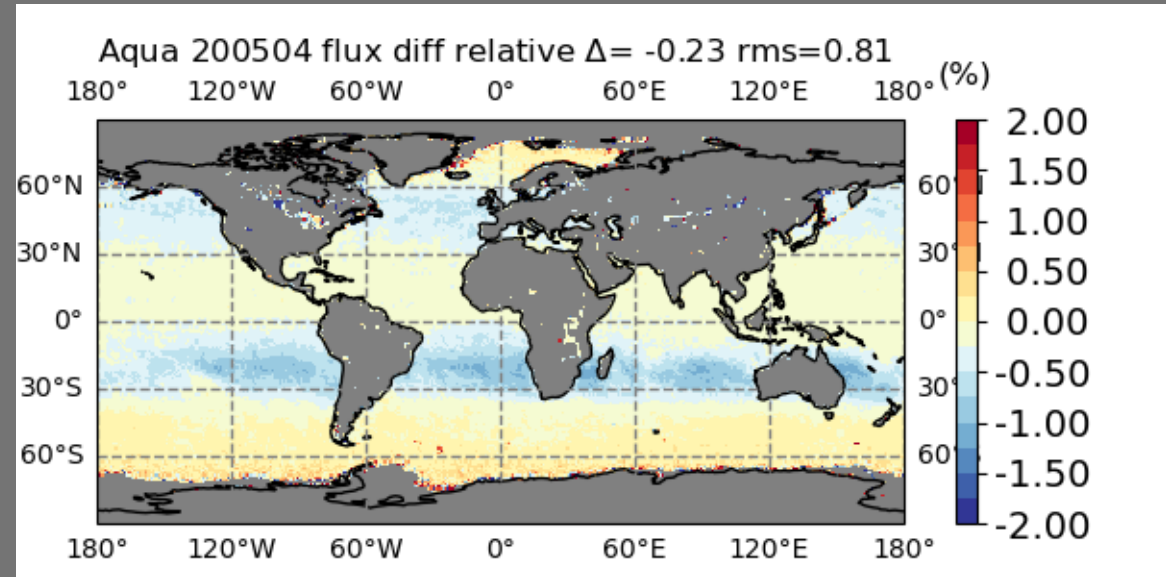


Cloudy-sky over ocean

Flux differences



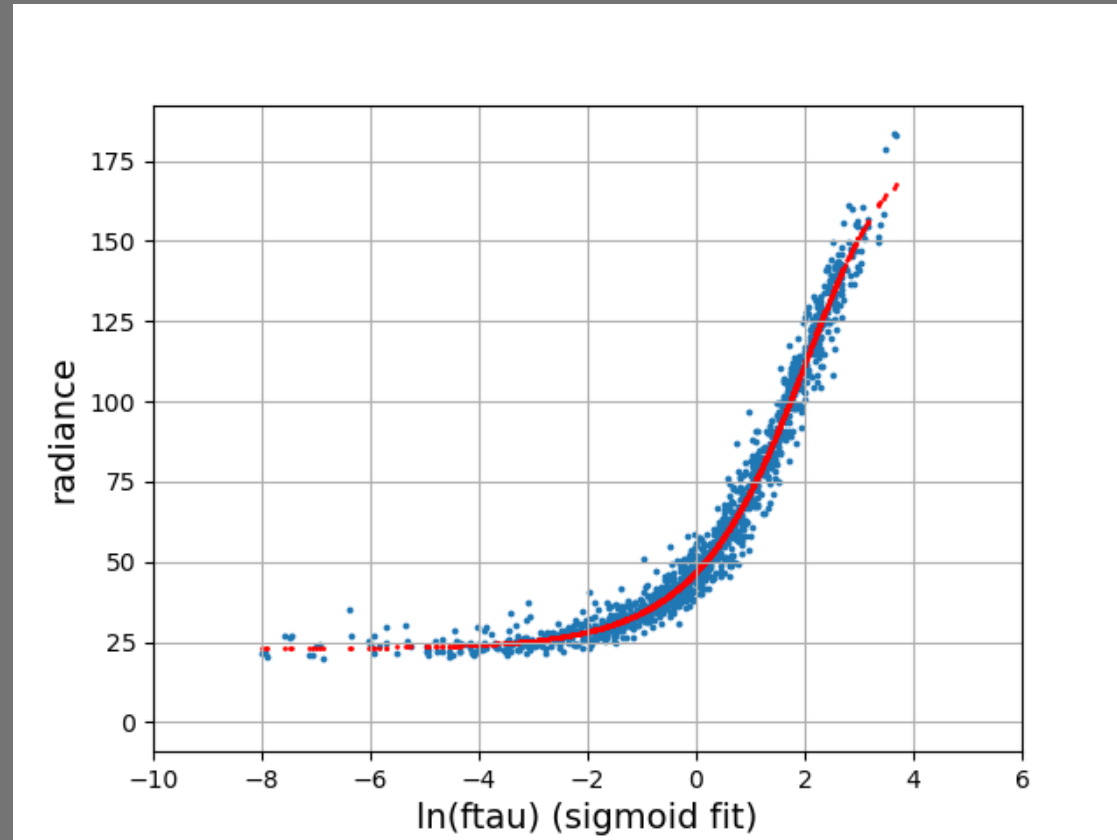
Flux Relative differences



Cloudy-sky over ocean

Processing of cloud-sky over ocean ADMs

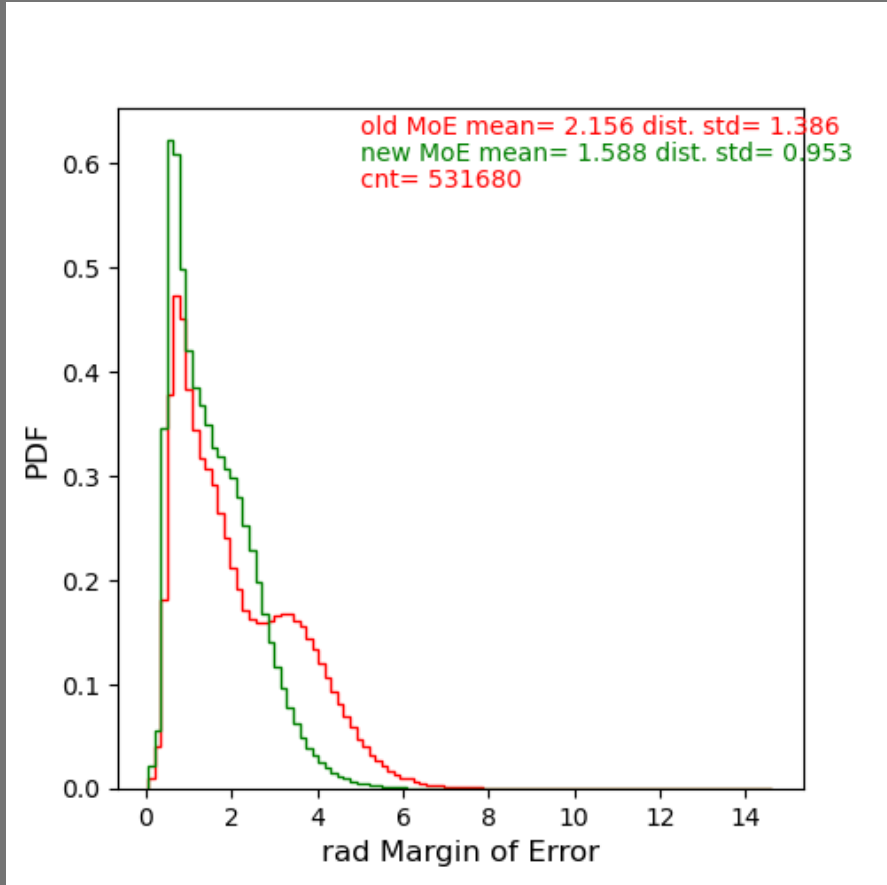
In a given angular bin, radiances are averaged in $\ln(f\tau)$ intervals, and sigmoid fit is used to relate the mean radiances and $\ln(f\tau)$ bin values.



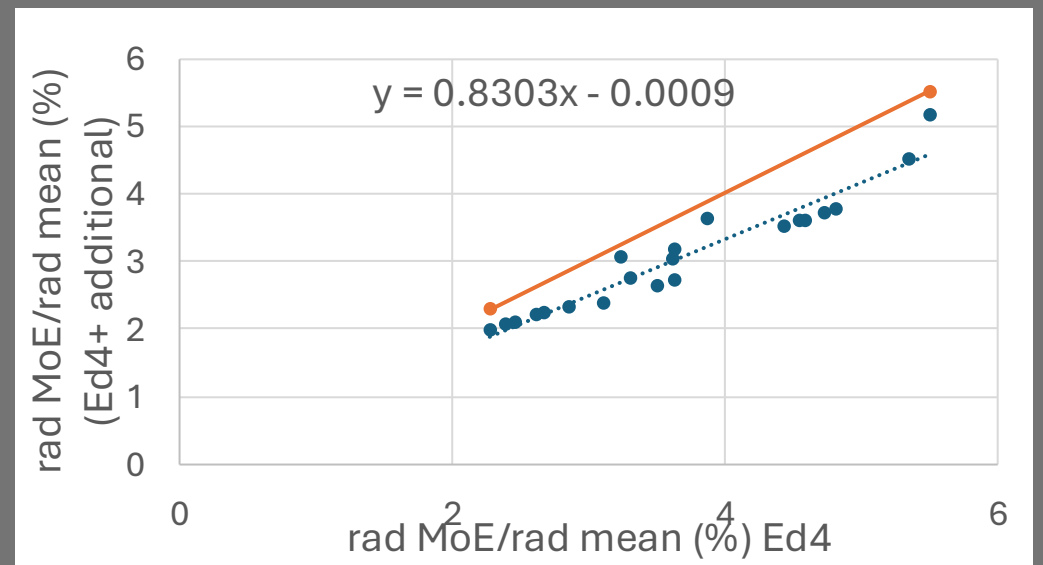
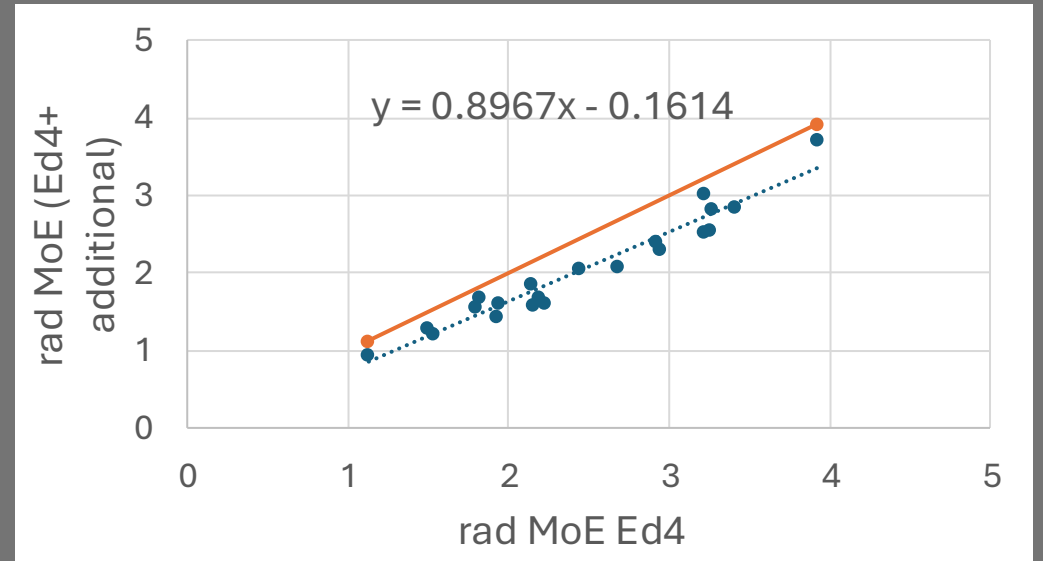
SZA=38-40, VZA=66-68 and RAZ=68-70 for water clouds
 f is the cloud fraction and τ is the cloud optical depth.

Cloudy-sky over ocean

Collect the mean MoE values from MoE distributions for 7 SZA bin intervals from 15 to 71 for water, mix and ice clouds.

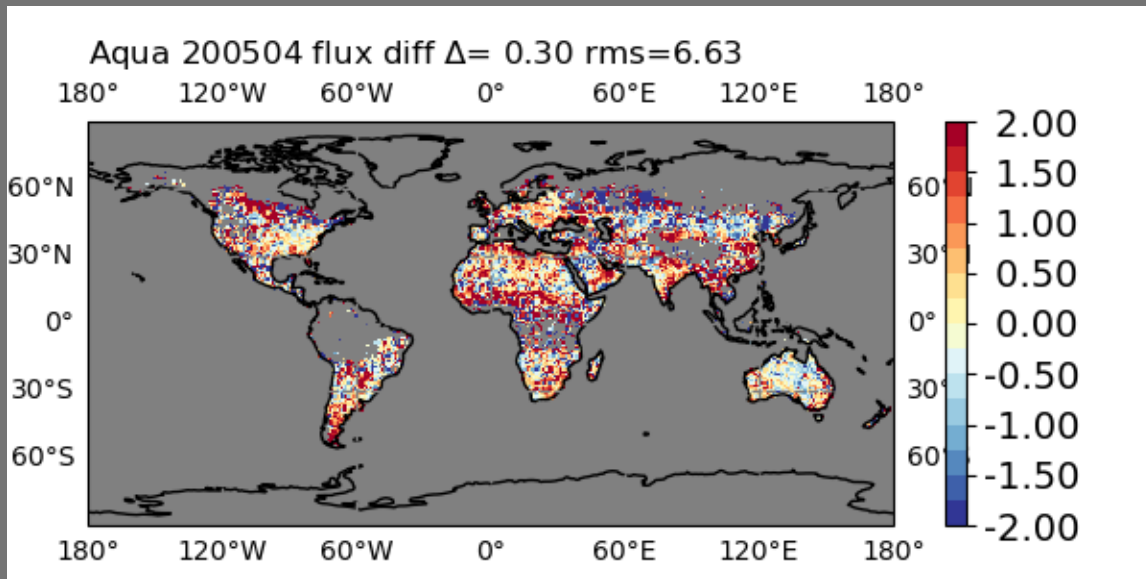


MoE distribution of optically thick clouds for viewing angles and $\ln(\text{ftau})$ bins (45 VZA \times 90 RAZ \times 775 $\ln(\text{ftau})$) for solar zenith angle = 38-40 and within non-glint region.

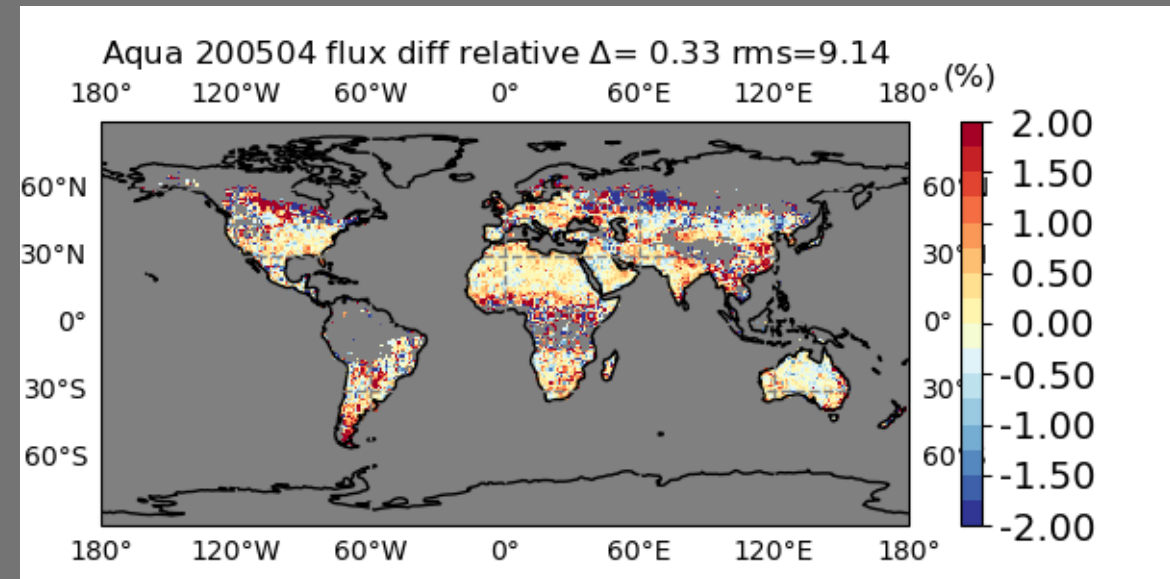


Clear-sky over land

Flux differences

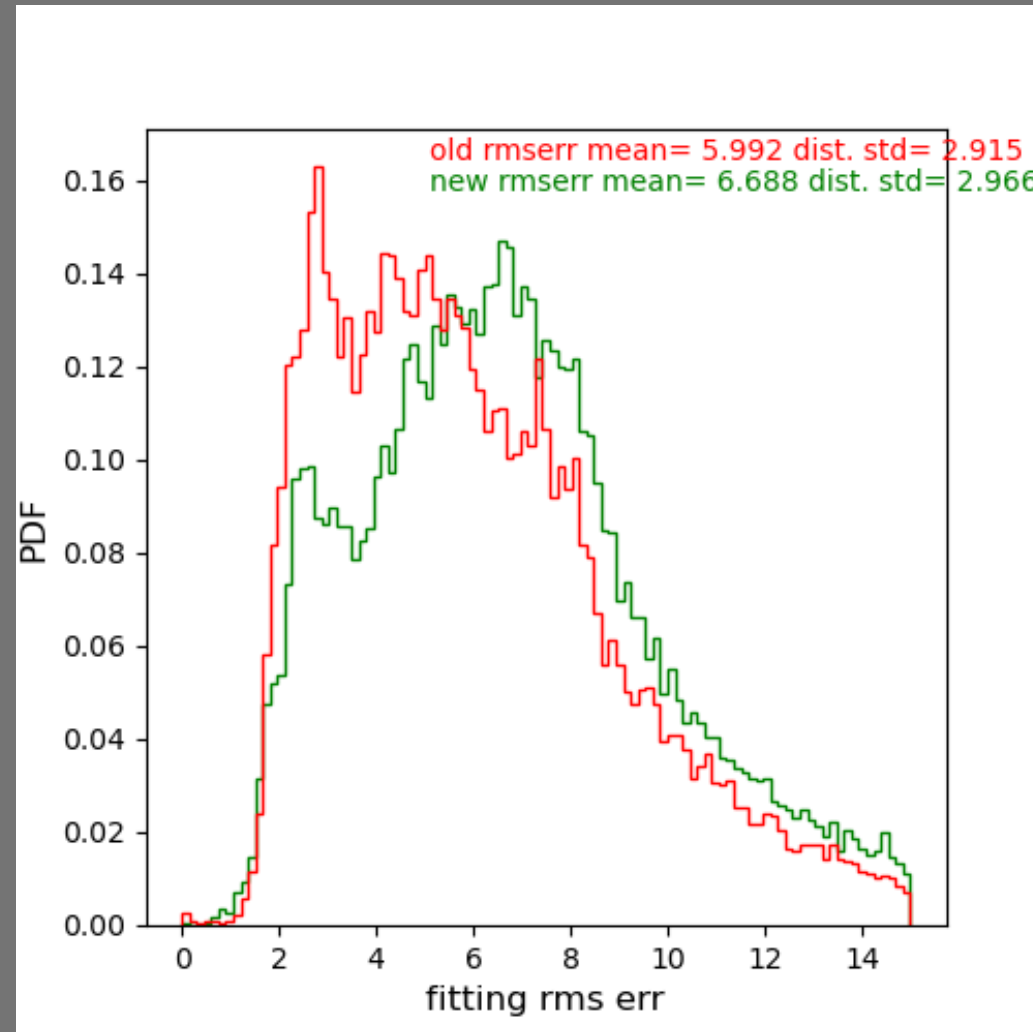


Flux Relative differences



Processing of clear-sky over land ADMs

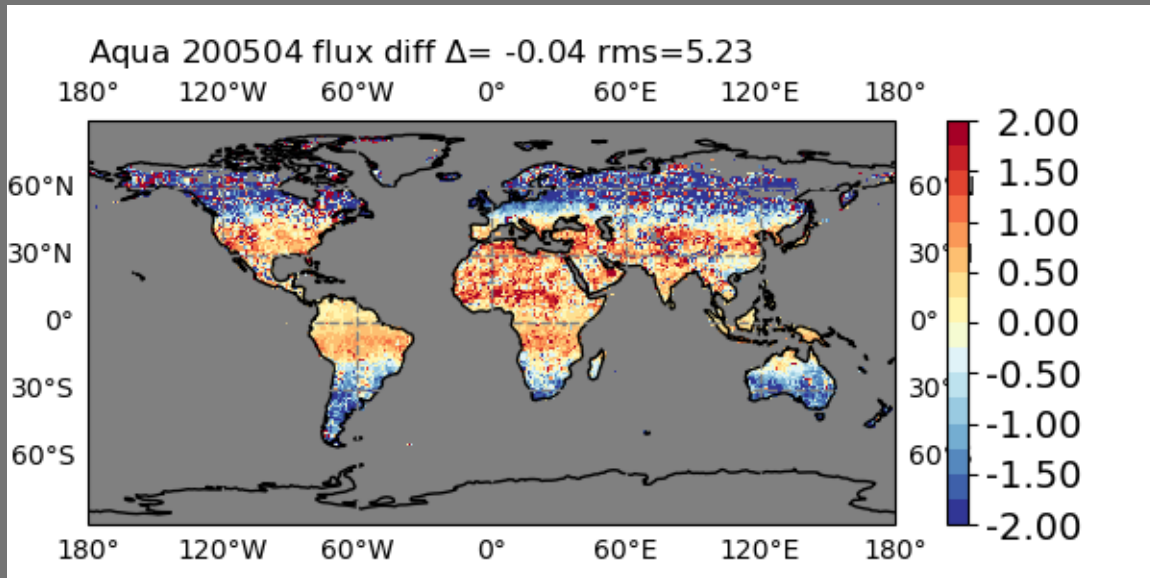
Within a SZA-NDVI bin interval, all observed radiances are used directly to fit the RossLi surface BRDF model. There is no radiance averaging involved.



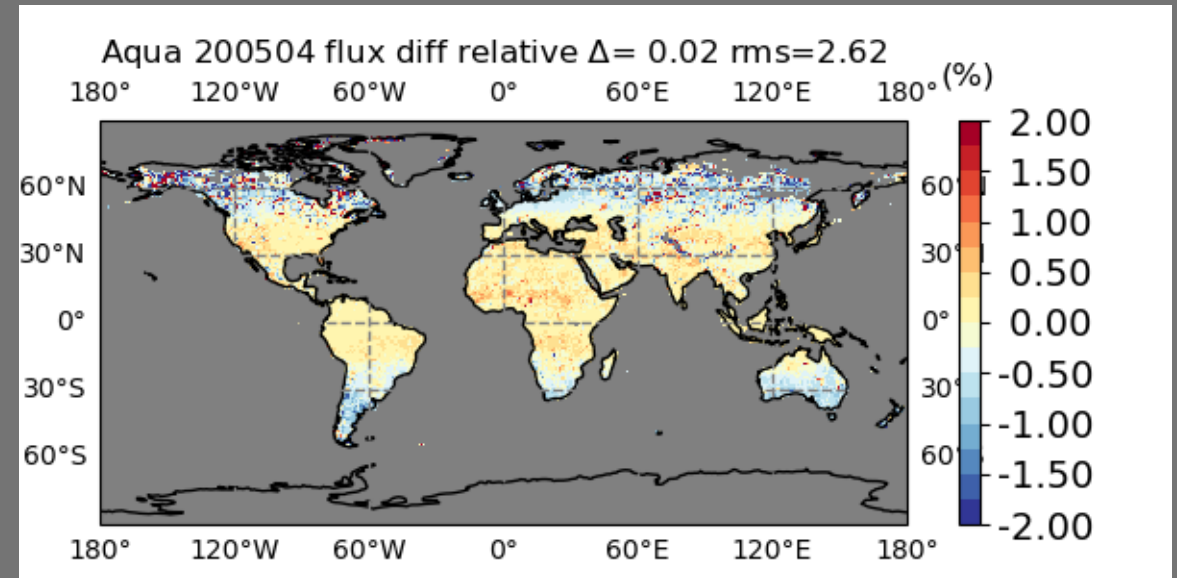
Fitting RMS errors for July

Cloudy-sky over land

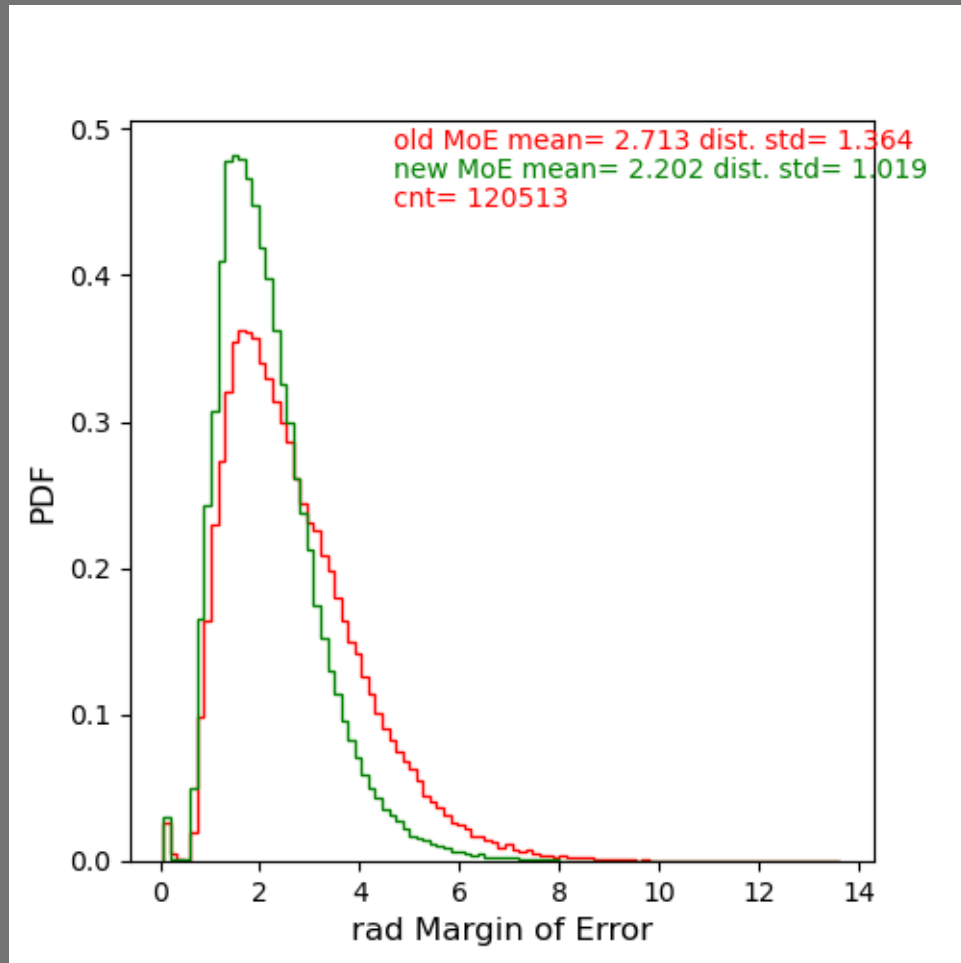
Flux differences



Flux Relative differences

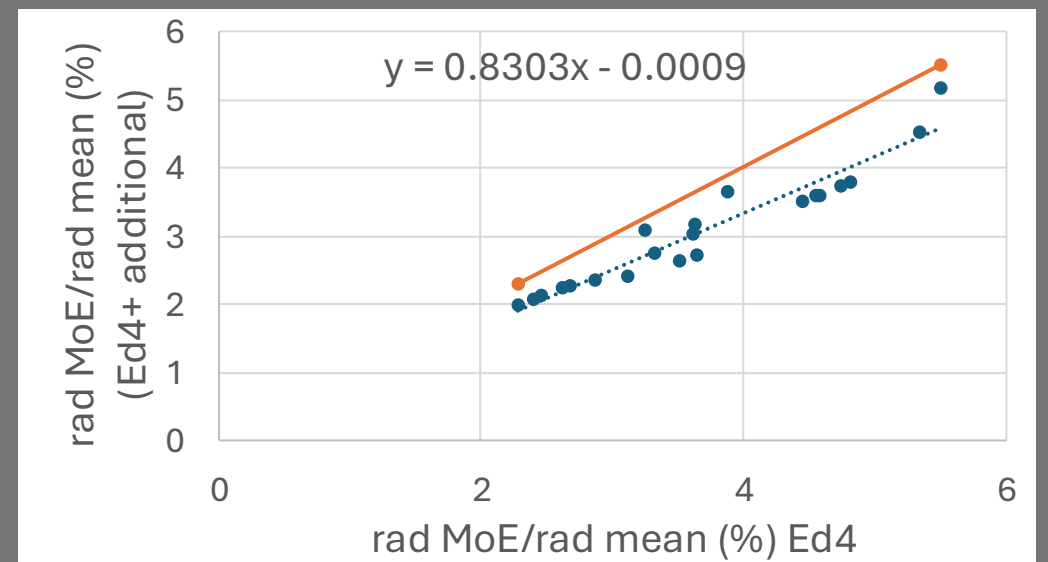
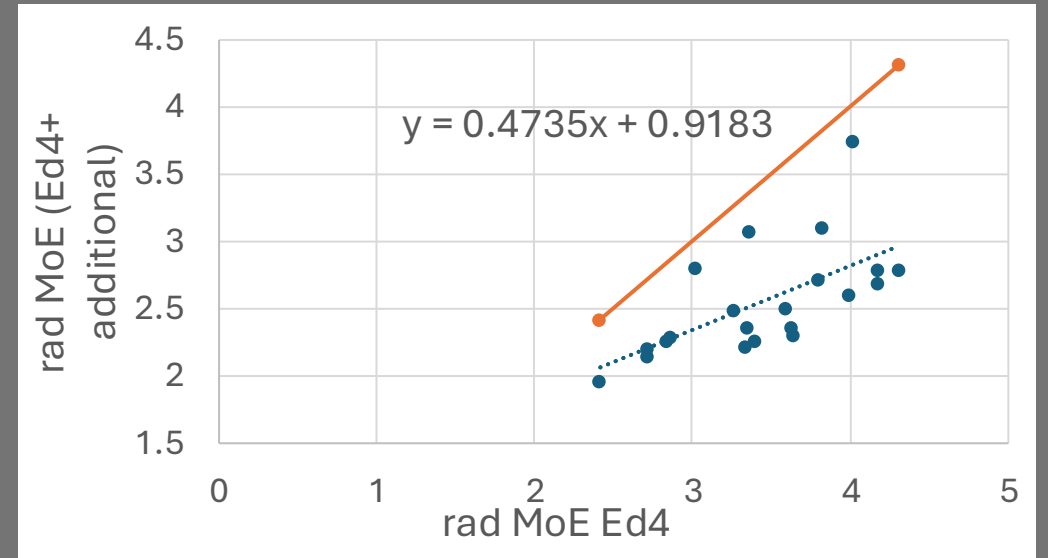


Cloudy-sky over land

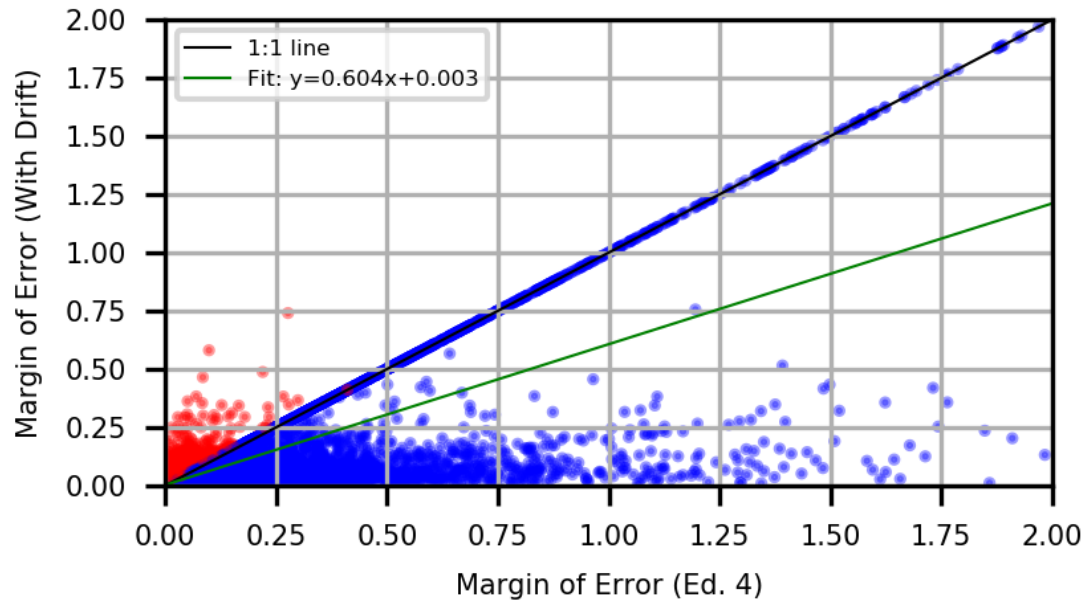


MoE distribution of water clouds for viewing angles and $\ln(\text{ftau})$ bins (18 VZA \times 36 RAZ \times 380 $\ln(\text{ftau})$) for solar zenith angle=25-30.

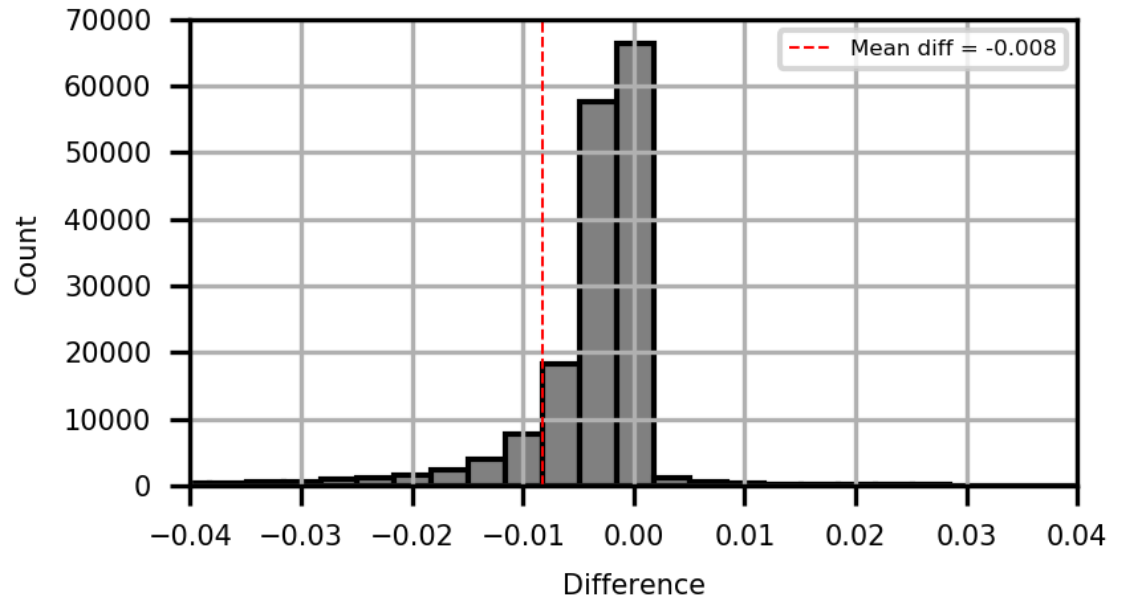
Collect the mean MoE values from MoE distributions for 7 SZA bin intervals from 17.5 to 77.5) for water, mix and ice clouds



Reflectance Margin of Error within ADM Bins



Histogram of Margin of Error Differences

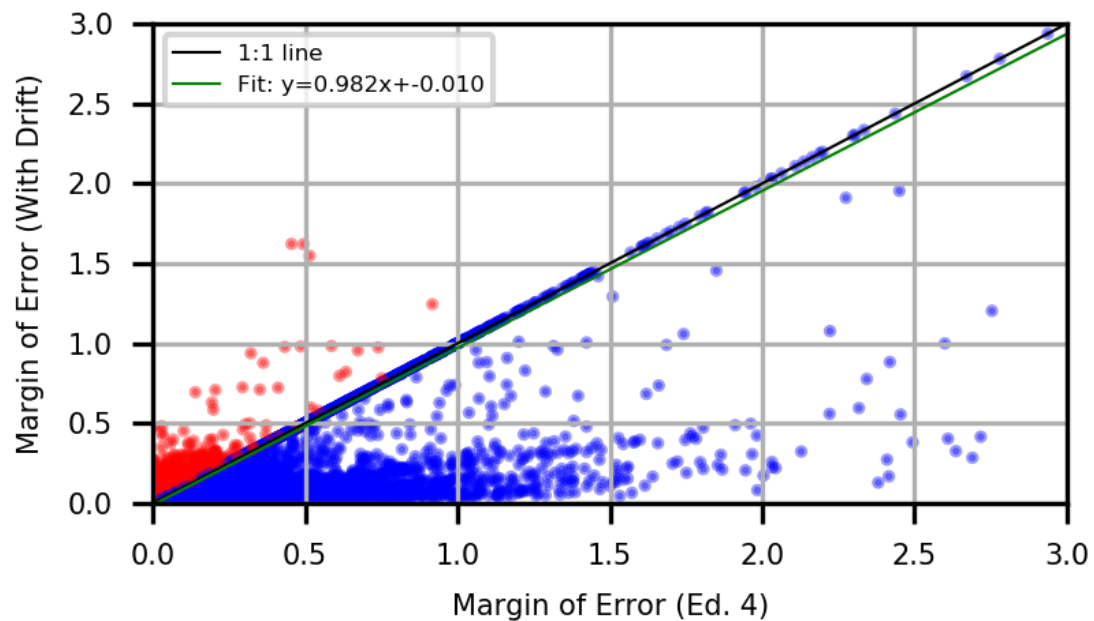


Cloudy Fresh Snow

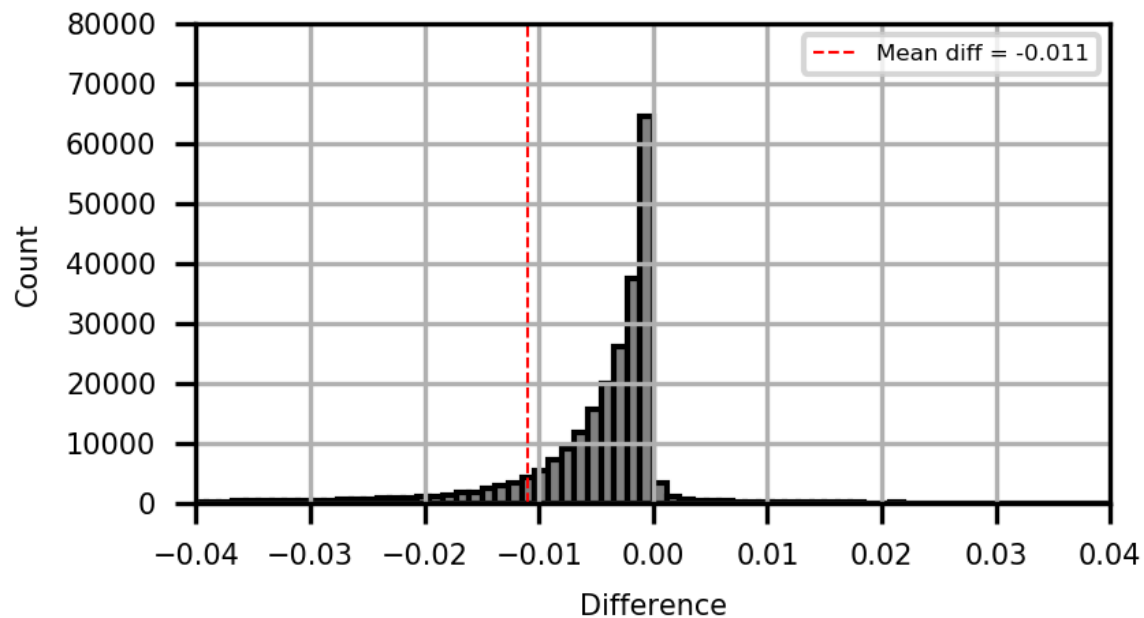
STATISTICAL SUMMARY

Slope:	0.6041
Intercept:	0.0026
Correlation (r):	0.8033
Confidence Interval:	0.95
Mean diff:	-0.0082
Median diff:	-0.0021
% above 1:1:	3.60%
% below 1:1:	89.26%

Reflectance Margin of Error within ADM Bins



Histogram of Margin of Error Differences



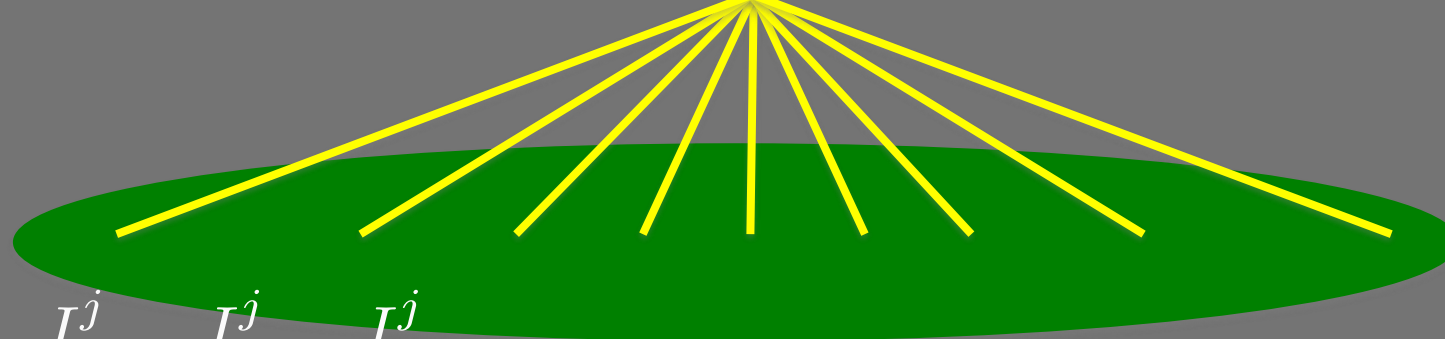
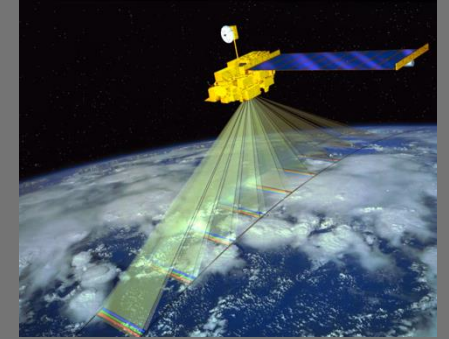
Partly Cloudy Sea Ice

STATISTICAL SUMMARY

Slope:	0.9819
Intercept:	-0.0103
Correlation (r):	0.9923
Confidence Interval:	0.95
Mean diff:	-0.0109
Median diff:	-0.0027
% above 1:1:	4.03%
% below 1:1:	90.04%

SW Flux Consistency (MISR)

For Terra CERES along track observations, collocated MISR footprints provide spectral radiance measurements from nine camera angles



$$I_{0.45}^j, I_{0.67}^j, I_{0.87}^j$$

$$I_{sw}^j = c_0 + c_1 I_{0.45}^j + c_2 I_{0.67}^j + c_3 I_{0.87}^j$$

↓ CERES ADM

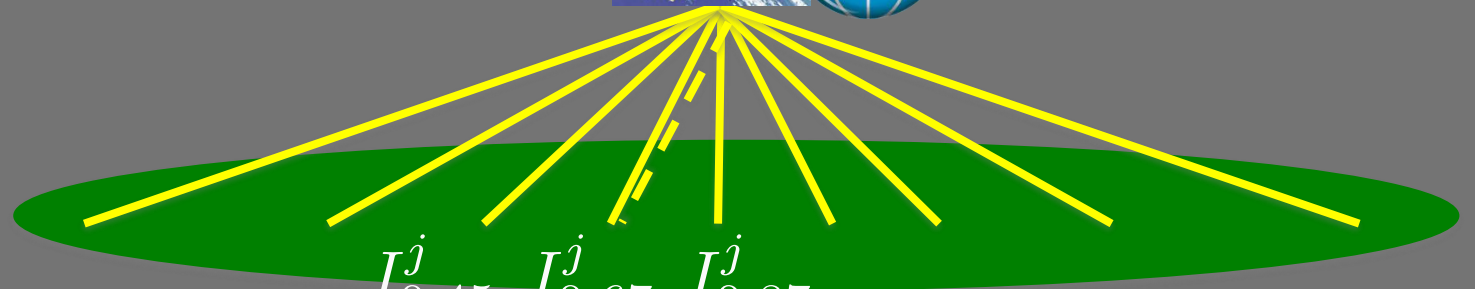
$$F_{sw}^j \longrightarrow \overline{F_{sw}} = \frac{\sum_{j=1}^9 F_{sw}^j}{9} \longrightarrow s = \sqrt{\frac{\sum_{j=1}^n (F_{sw}^j - \overline{F_{sw}})^2}{n-1}}$$

For M CERES footprints, the total relative consistency is:

$$CV_T = \left(\frac{\sqrt{\frac{1}{M} \sum_{i=1}^M s_i^2}}{\frac{1}{M} \sum_{i=1}^M F_{sw}^i} \right) \times 100\%$$

It quantifies

1. how well the CERES SW ADMs represent the anisotropy of a scene and
2. the accuracy in the narrow-to-broadband regression.



$$I_{0.45}^j, I_{0.67}^j, I_{0.87}^j$$

$$I_{sw}^c \quad I_{sw}^j = c_0 + c_1 I_{0.45}^j + c_2 I_{0.67}^j + c_3 I_{0.87}^j$$

CERES ADM

$$F_{sw}^c \quad F_{sw}^j$$

$$CV_{NB} = \left(\frac{\sqrt{\frac{1}{m} \sum_{i=1}^m (F_{sw}^j - F_{sw}^c)^2}}{\frac{1}{m} \sum_{i=1}^m F_{sw}^c} \right) \times 100\%$$

$$CV_{ADM} = \sqrt{CV_T^2 - CV_{NB}^2}$$

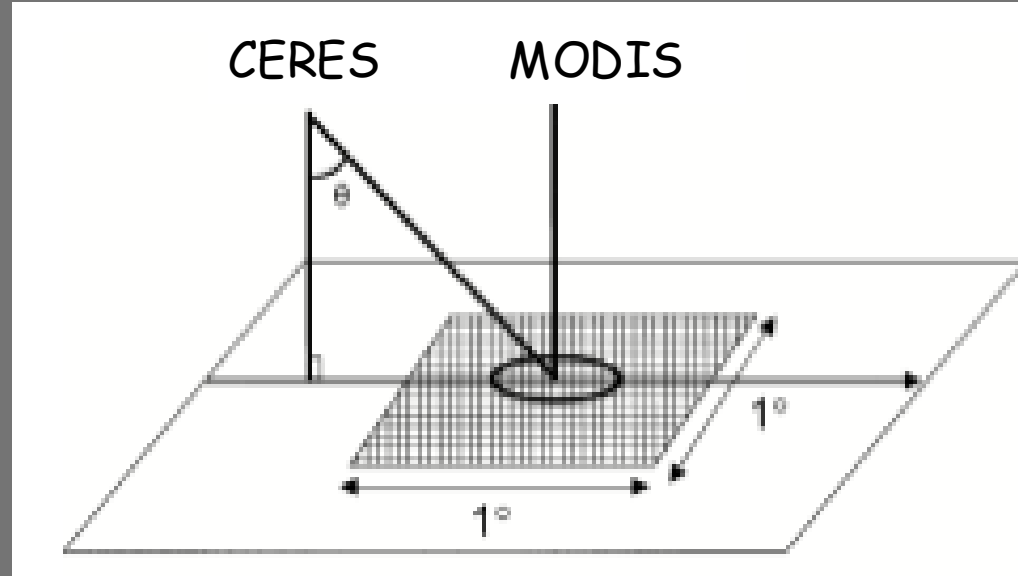
SW Flux Consistency (MISR)

CERES-MISR SW Flux Consistency Test for Terra during period May 2000 - February 2005

	Ocean				Land				Snow/Ice			
	Clear	S	M	All	Clear	S	M	All	Clear	S	M	All
N	200	200	200	200	25	50	50	50	50	50	50	50
$\Psi_{ADM}^{No_Drift}$ (%)	3.28	4.62	8.41	6.19	2.04	4.94	6.56	3.99	4.77	6.26	5.92	5.92
Ψ_{ADM}^{Drift} (%)	3.28	4.62	8.41	6.19	2.02	4.93	6.51	3.97	4.72	6.18	5.93	5.86

S: single layer clouds; M: multiple-layer clouds

SW Flux Consistency (MODIS)



1. For CERES along-track observations, CERES viewed a footprint @60 VZA and MODIS viewed it near nadir for the same footprint.
2. Convert MODIS narrow-band radiances $R_{\text{MOD_NB}}$, to broad-band radiances $R_{\text{MOD_BB}}$. Retrieve flux based on $R_{\text{MOD_BB}}$ with MODIS viewing-geometries, treating it like CERES observations.
3. Compare $F_{\text{MOD_BB}}$ (near nadir) and $F_{\text{CERES_BB}}$ (@60 VZA).

SW RMS errors between $F_{\text{MOD_BB}}$ (near nadir) and $F_{\text{CERES_BB}}$ (@60 VZA)

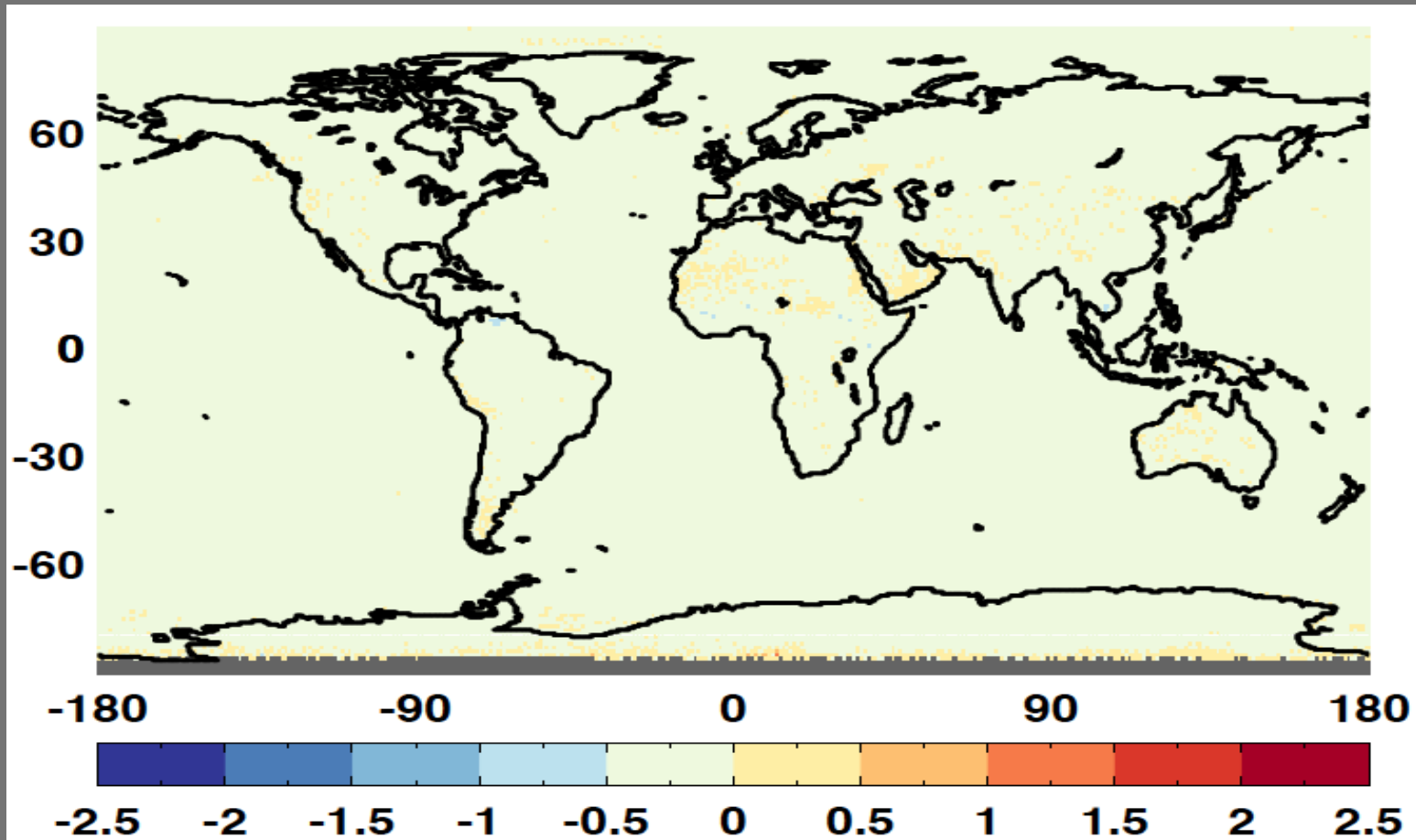
Ocean RMS error (%)		
	Ed4	Ed4 + additional RAPs
clear	4.4	4.3
single-layer	5.2	5.2
Multiple-layer	9.7	9.7
all	6.0	6.0

Land RMS error (%)		
	Ed4	Ed4 + additional RAPs
clear	3.8	3.8
single-layer	6.0	6.0
Multiple-layer	8.4	8.3
all	5.9	5.9

LW flux differences (all-sky)

Aqua 201504 Daytime

Avg diff: -0.16 W m^{-2} RMS diff: 0.18 W m^{-2}



LUT approach for split SW flux retrieval

Visible flux from Libera

- Incoming energy in the range from 0.3-5.0 μm can be split by VIS (0.3-0.7 μm) and NIR (0.7-5.0 μm).
- Libera has a split-shortwave channel (NIR: 0.7-5 μm), in addition to the traditional shortwave (0.3-5 μm), longwave (5-50 μm), and total (0.3-100 μm) channels.

$$I_{VIS} = I_{SW} - I_{NIR}$$

- Radiances in the visible band (0.3-0.7 μm) is:

$$F_{VIS} = R(I_{VIS})$$

- F_{VIS} can be converted from I_{VIS} if visible ADMs are available.

Alternative approach for split SW flux retrieval

- Define an anisotropic factor ratio of NIR to VIS

$$\beta = R_{\text{NIR}} / R_{\text{VIS}}$$

- The NIR flux relates to SW flux by

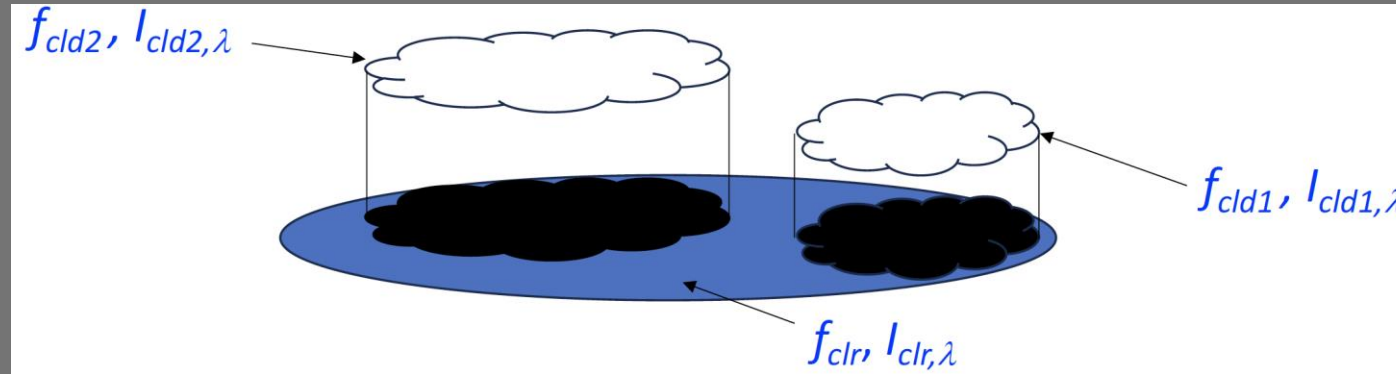
$$F_{\text{NIR}} = \frac{F_{\text{SW}}}{1 + \alpha}, \quad \text{where, } \alpha = \frac{F_{\text{VIS}}}{F_{\text{NIR}}} = \left(1 + \frac{I_{\text{VIS}}}{I_{\text{NIR}}} \beta \right),$$

- The VIS flux is then determined by

$$F_{\text{VIS}} = F_{\text{SW}} - F_{\text{NIR}}$$

- β is retrieved from radiative transfer model LUTs by minimizing the errors between simulated and observed narrow-band radiances.
- Currently, I_{VIS} and I_{NIR} are derived from ratios to I_{SW} based on theoretical simulations to calculate $\alpha = (I_{\text{VIS}} / I_{\text{NIR}}) \beta$, respectively.

Matching of narrow-band simulations and observations



- Matching spectral simulations to the observations for each sub-footprint, then calculate the total footprint $I'_{VIS}, I'_{NIR}, F'_{VIS}, F'_{NIR}$ by area-weighting sub-footprint values:

$$I'_x = [f_{clr}I'_{clr,x} + f_{cld1}I'_{cld1,x} + f_{cld2}I'_{cld2,x}] / (f_{clr} + f_{cld1} + f_{cld2})$$

$$F'_x = [f_{clr}F'_{clr,x} + f_{cld1}F'_{cld1,x} + f_{cld2}F'_{cld2,x}] / (f_{clr} + f_{cld1} + f_{cld2})$$

- Anisotropic factors for visible and NIR can be derived from $I'_{VIS}, I'_{NIR}, F'_{VIS}, F'_{NIR}$.

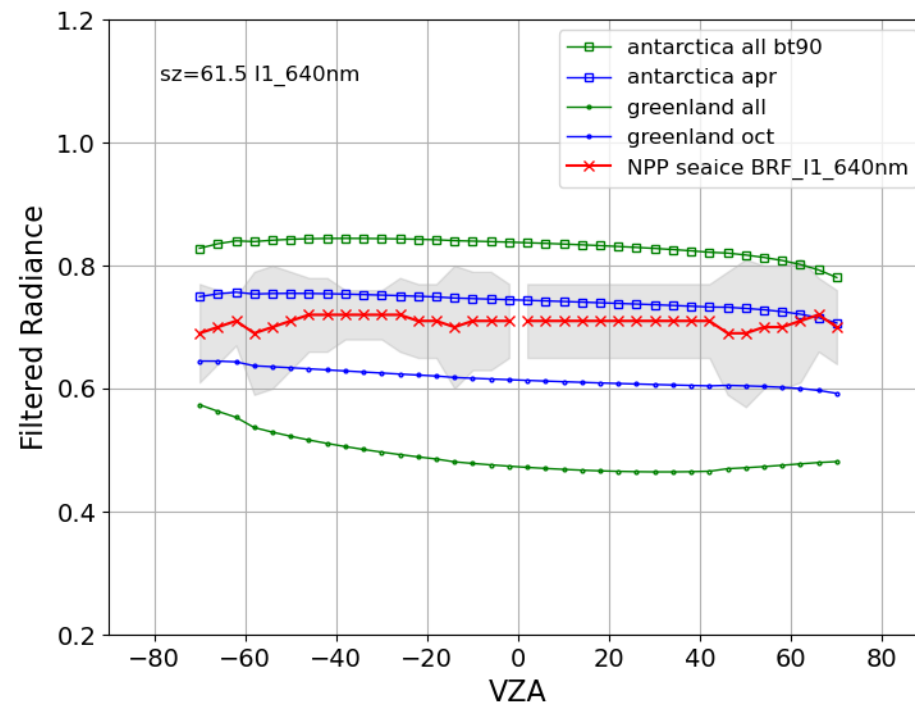
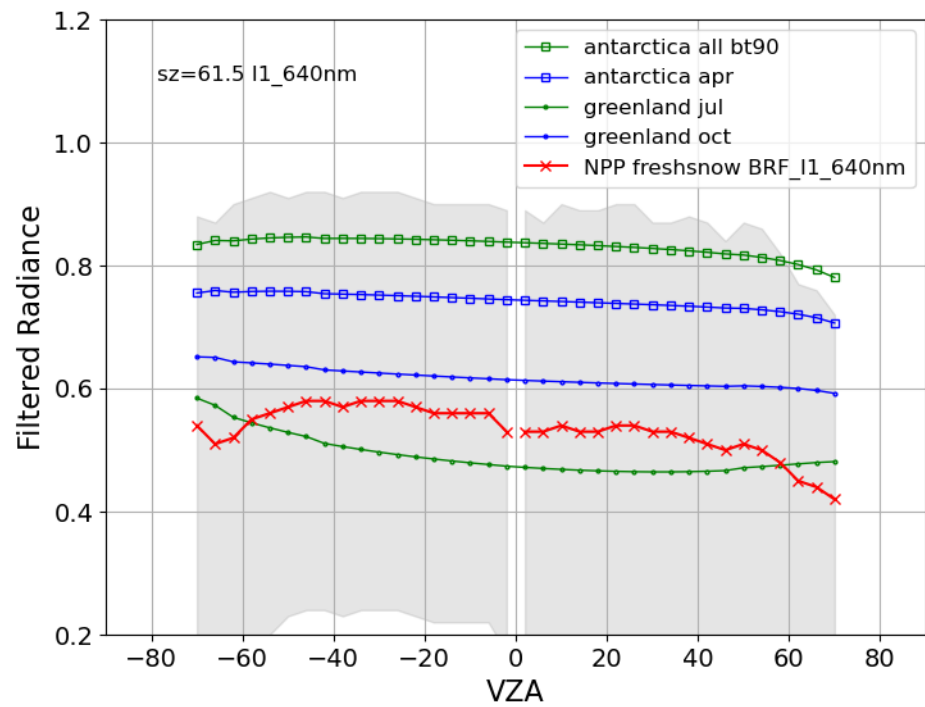
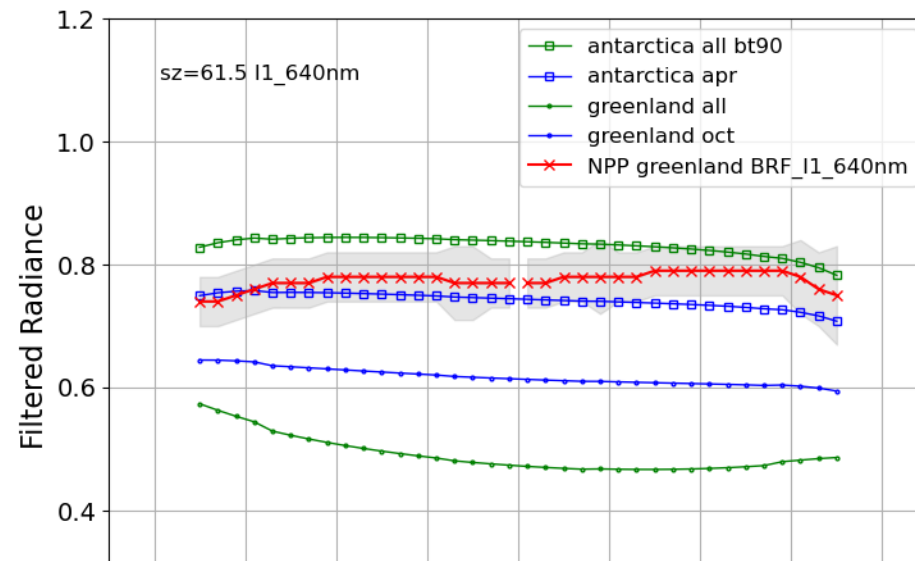
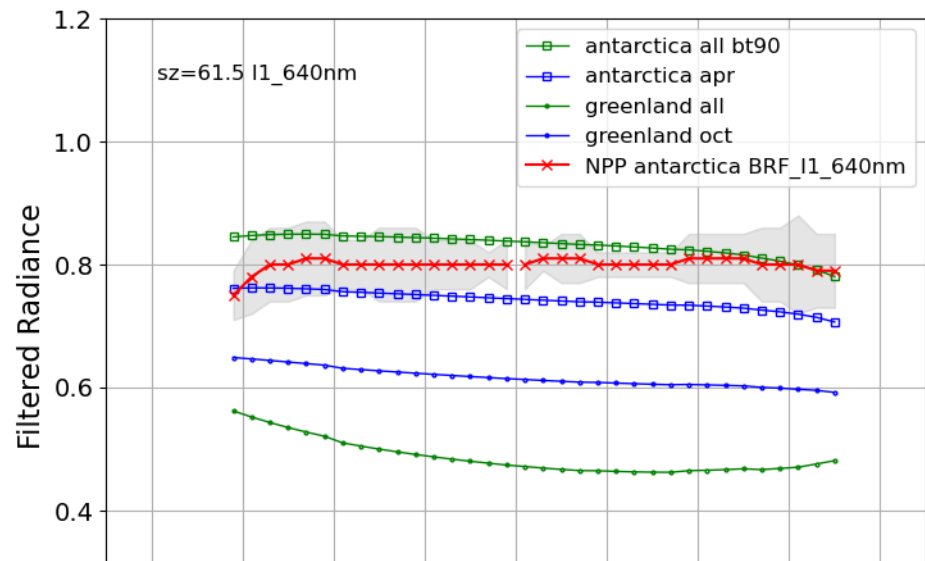
$$R_x = \pi I'_x / F'_x$$

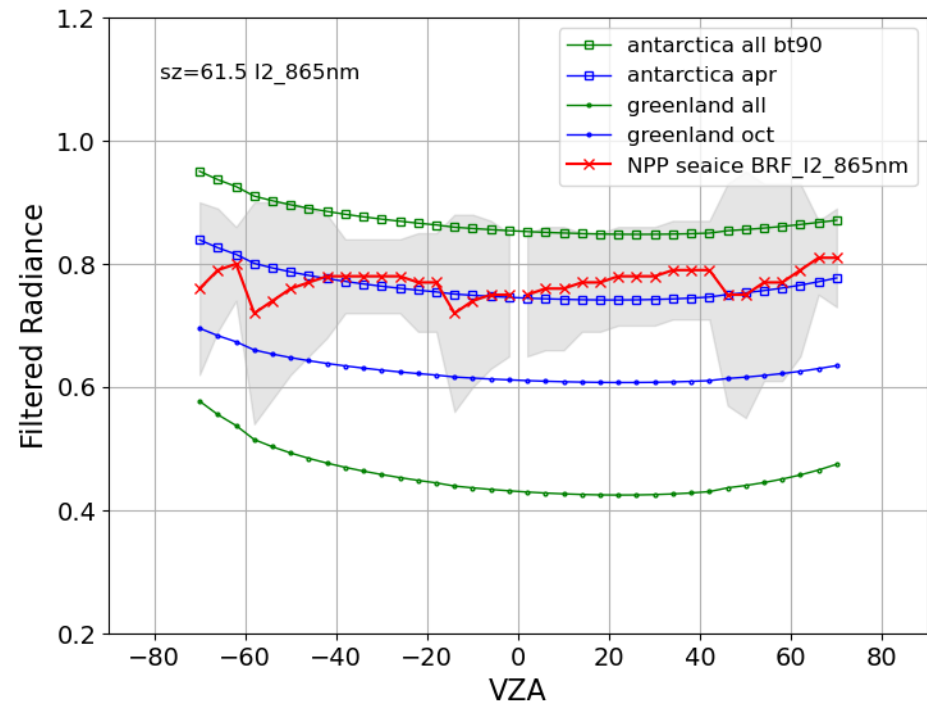
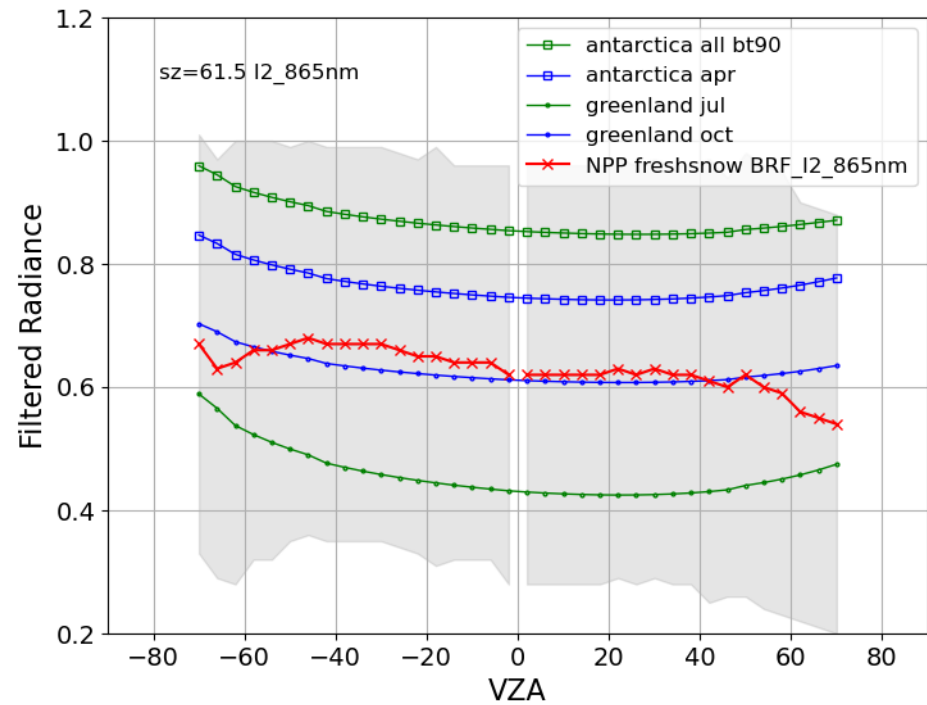
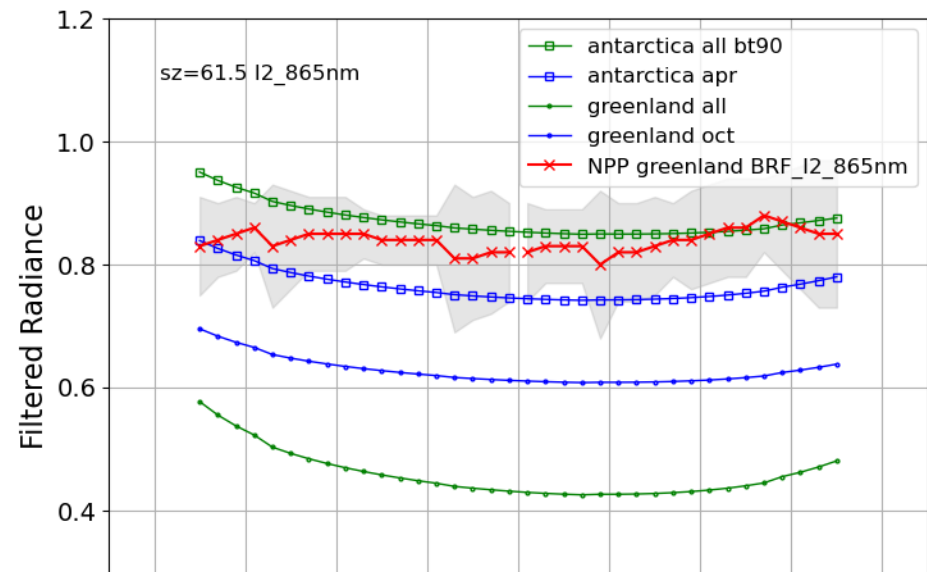
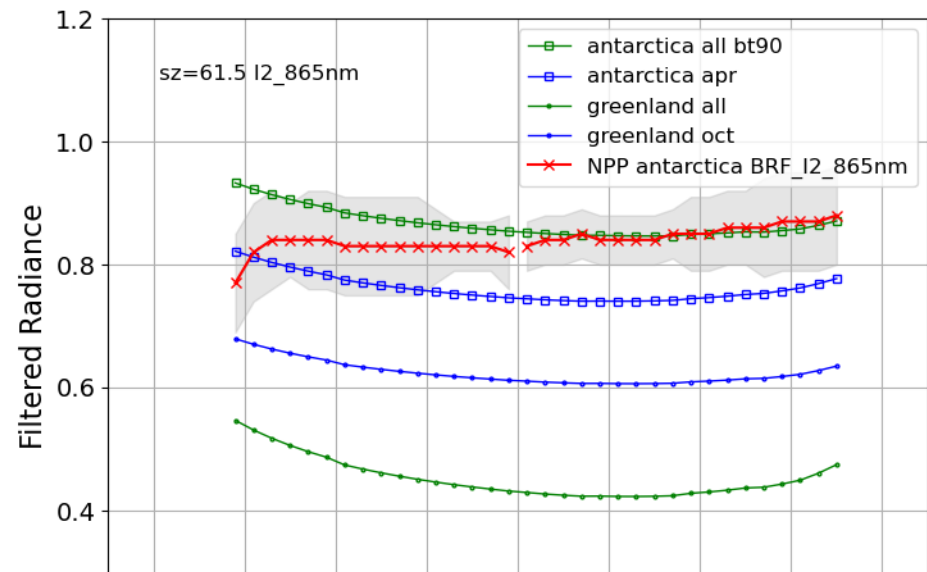
- Retrieve $\beta = (R_{NIR} / R_{VIS})$

MODTRAN simulations for β retrieval LUTs

β retrieval LUTs contain members according to sensitivity of β to scene Properties (e.g., cloud optical depth, aerosols, surface BRDF, etc.)

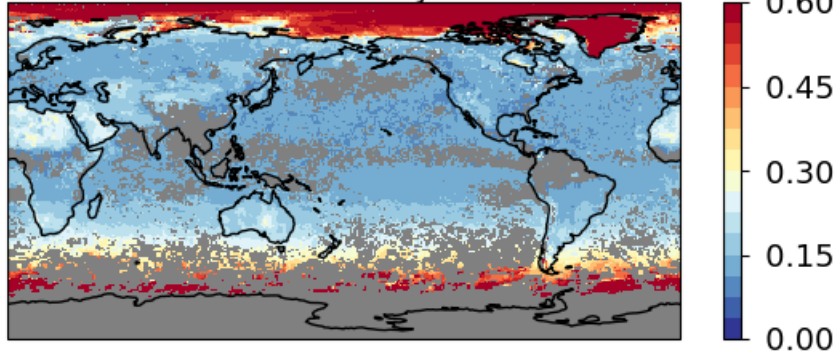
- Clear sky over ocean
 - 6 AODs, 2 ocean wind speeds
- Clear sky over land
 - 4 surface types characterized by MODIS RossLi BRDF models in the season of JJA and DJF, respectively, and 3 AODs
- Clear sky over snow/ice
 - 4 surface types to characterize permanent snow (Greenland and Antarctica), sea-ice, and fresh snow
- Overcast
 - 6 CODs and 2 cloud phases.



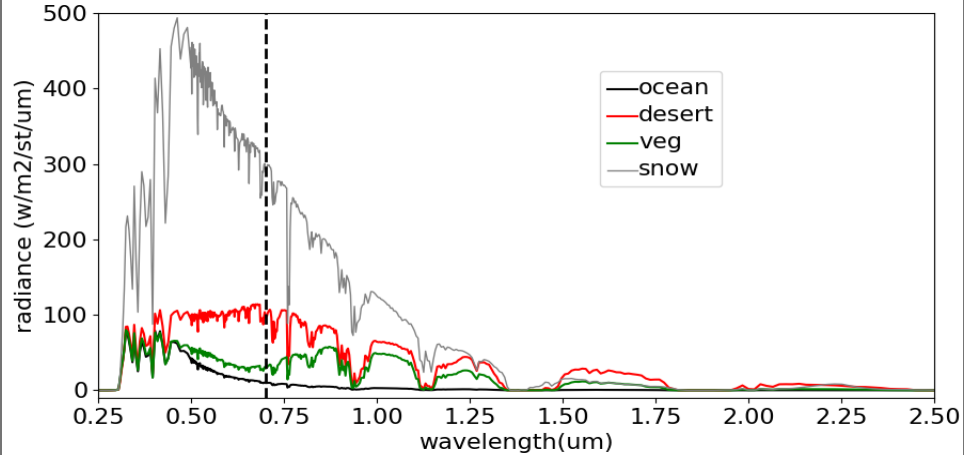
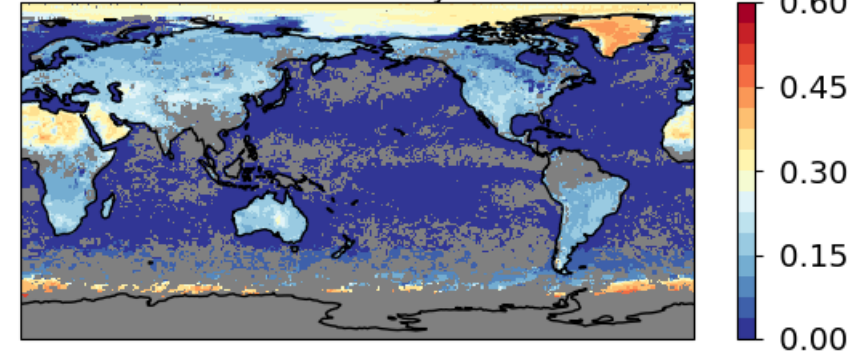


Clear sky

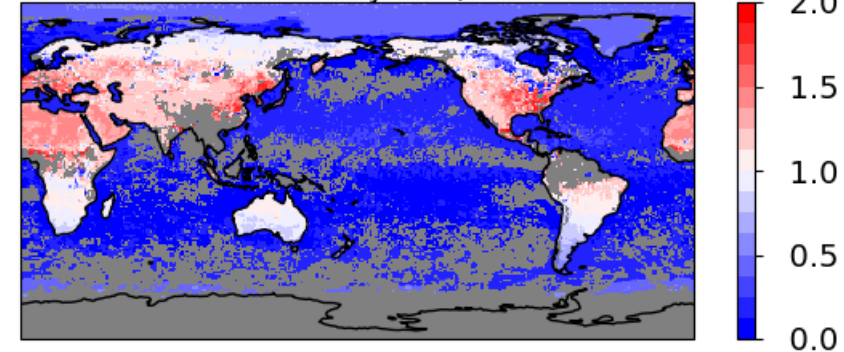
201407 NPP-FM5 VIS clrsky alb



201407 NPP-FM5 NIR clrsky alb



201407 NPP-FM5 clrsky Anir/Avis



VIS > NIR

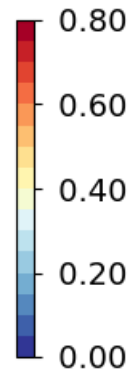
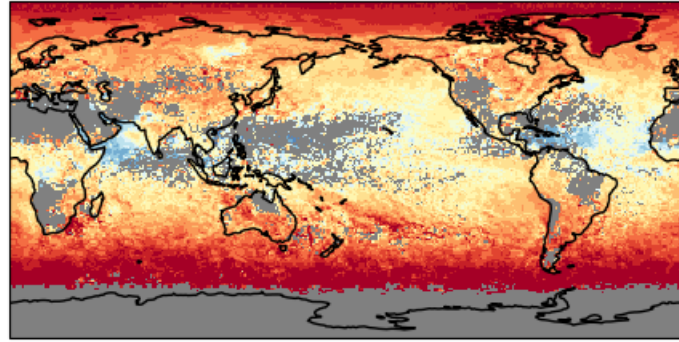
- **ocean**: high absorption by atmosphere and ocean water in the NIR spectral range
- **snow**: dominated by high reflectivity in the VIS spectral range and increased absorption in the NIR spectral range

VIS < NIR

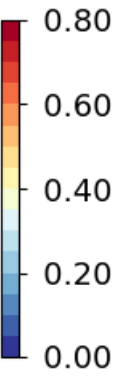
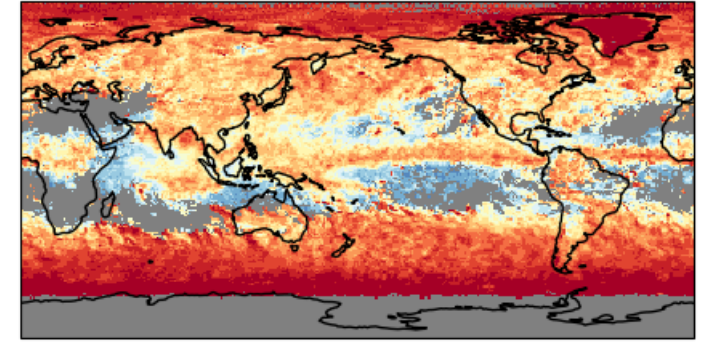
- **desert**: less absorption by dry atmosphere and higher reflectivity in the NIR spectral range.
- **vegetation**: high absorption in VIS spectral range for photosynthesis.

Overcast

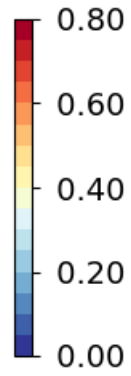
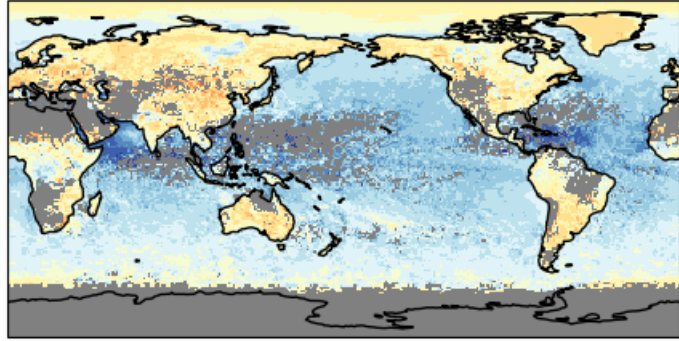
201407 NPP-FM5 VIS water ov alb



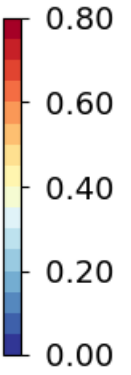
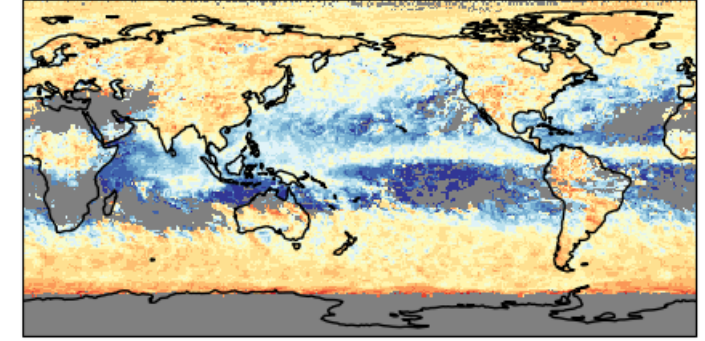
201407 NPP-FM5 VIS ice ov alb



201407 NPP-FM5 NIR water ov alb

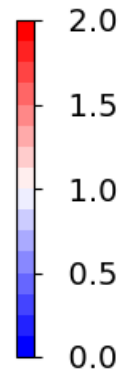
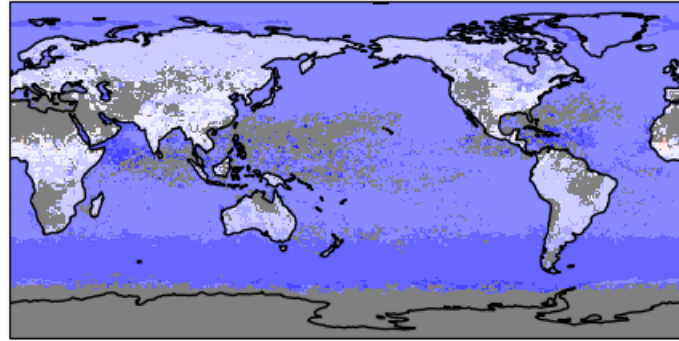


201407 NPP-FM5 NIR ice ov alb

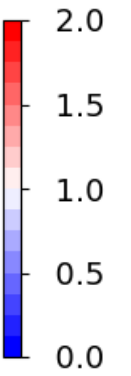
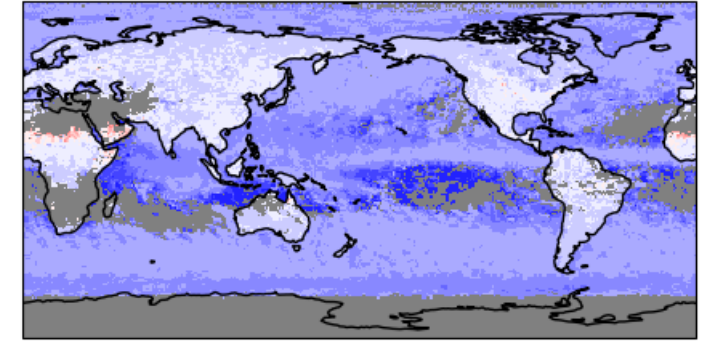


VIS > NIR: higher reflectivity of clouds in VIS than NIR range

201407 NPP-FM5 water ov Anir/Avis

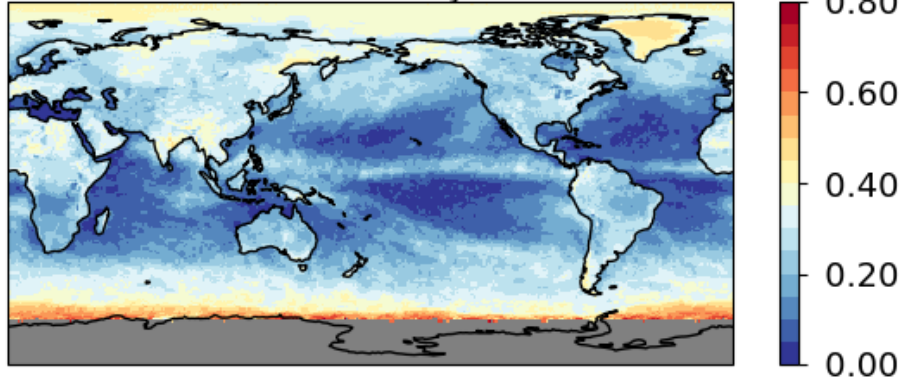


201407 NPP-FM5 ice ov Anir/Avis

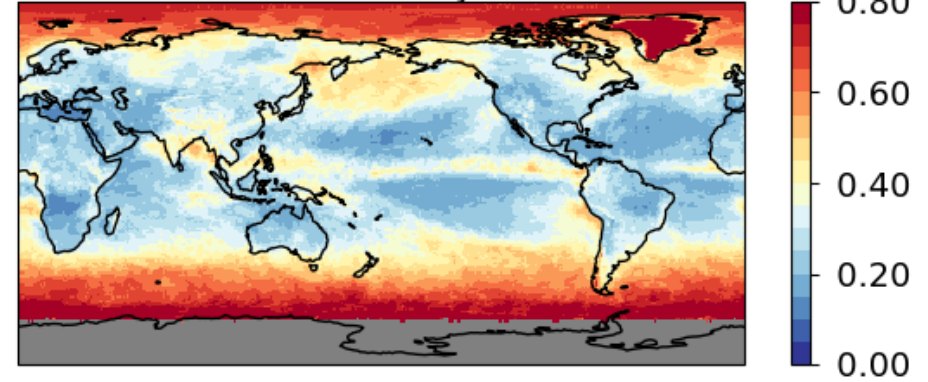


Comparison to CERES SYN calculation

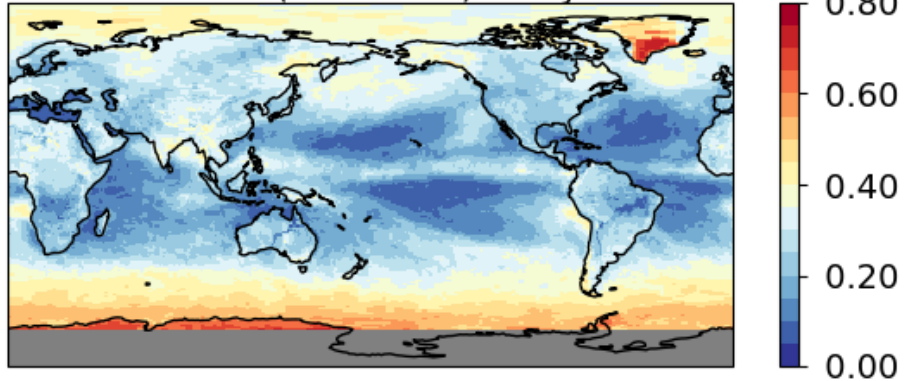
201407 NPP-FM5 NIR allsky alb



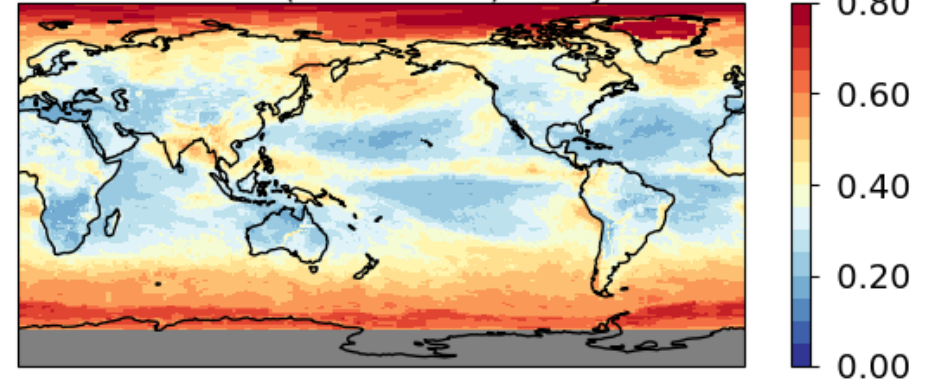
201407 NPP-FM5 VIS allsky alb



CERES SYN NIR (0.7-4.0um) allsky alb 201407



CERES SYN VIS (0.18-0.7um) allsky alb 201407



Summary

- Adding additional CERES RAPs observations during Terra/Aqua orbital drifting period reduced errors in mean radiances for LW and SW ADMs.
- Additional CERES RAPs observations during Terra/Aqua orbital drifting period increases coverage of radiance binned-means and thus improved CERES directional model.
- As expected, the LUT approach retrieved Clear-sky TOA VIS fluxes are greater than NIR fluxes over ocean and snow and smaller over desert and vegetation; and VIS fluxes are greater than NIR fluxes for overcast cloudy scenes.
- The LUT approach retrieved VIS and NIR albedos agree well with that by the CERES SYN model-based albedos, adding confidence to the validity of the method that we developed.